Volume 1
Number 2
March 2023
Pages 145–330

Sustainable Food Technology

rsc.li/susfoodtech

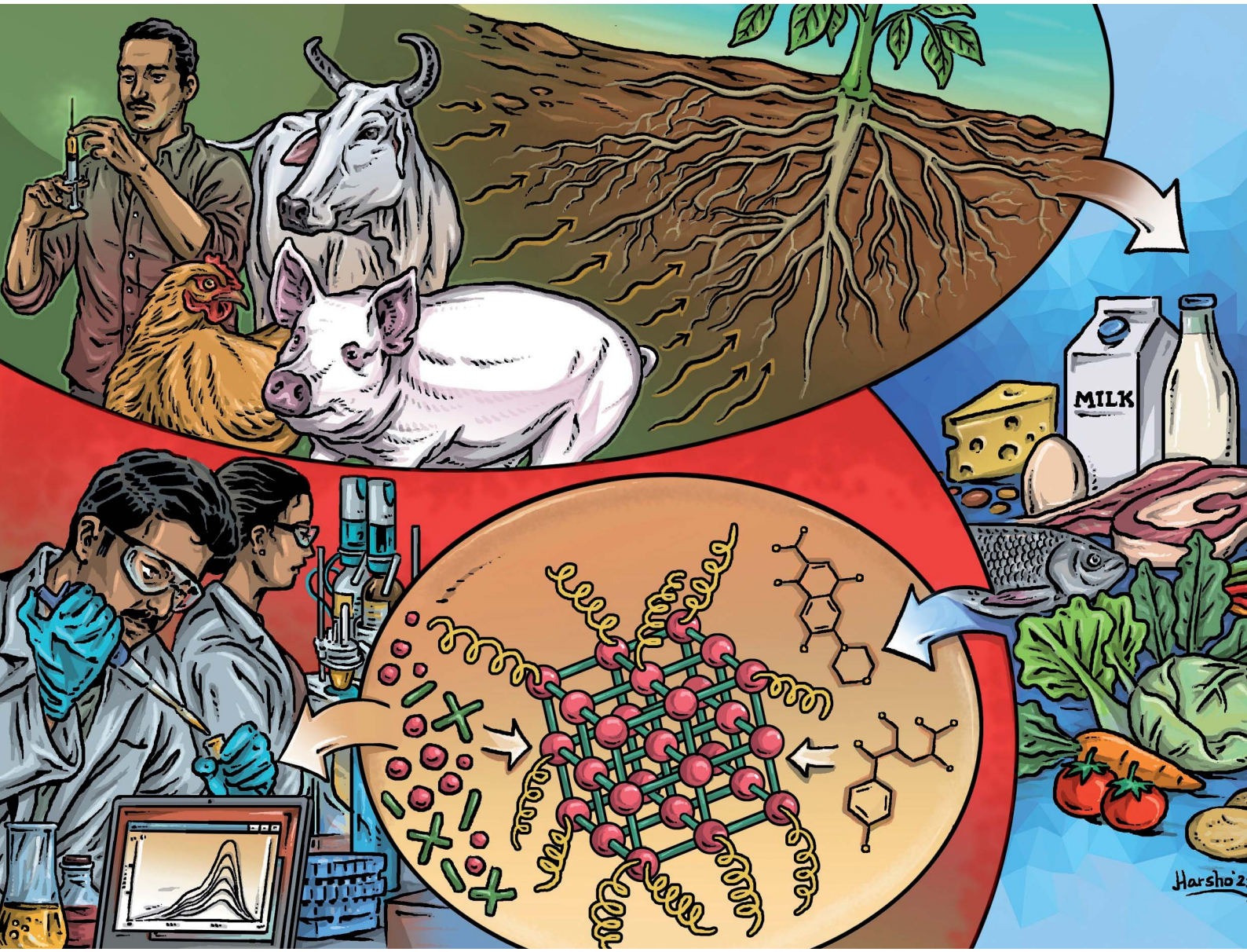

ISSN 2753-8095

ROYAL SOCIETY OF CHEMISTRY

REVIEW ARTICLE

P. Murali Krishna *et al.*

Advances and effectiveness of metal–organic framework based bio/chemical sensors for rapid and ultrasensitive probing of antibiotic residues in foods

Sustainable Food Technology

ROYAL SOCIETY OF CHEMISTRY

REVIEW

View Article Online
View Journal | View Issue

Cite this: *Sustainable Food Technol.*, 2023, **1**, 152

Advances and effectiveness of metal–organic framework based bio/chemical sensors for rapid and ultrasensitive probing of antibiotic residues in foods

Mirinal Kumar Rayappa,[a] Kavya K. S.,[a] Gurdeep Rattu[ab] and P. Murali Krishna *[a]

Antibiotic residues in foods are a global threat and one of the main reasons for the antibiotic resistance development in bacteria as reported by WHO and many other agencies. Antibiotics are used for the prevention and treatment of various diseases in humans and animals. They are employed to improve the growth rate and feed efficiency in livestock predominantly. The global antibiotic usage in food animals including aquaculture is increasing rapidly and is estimated to increase by 67% by 2030. Due to a lack of adherence to proper dosage protocols, various antibiotic residues have become increasingly prevalent in food products obtained from livestock that are meant for human consumption. Moreover, these complex antibiotic residues can cause chronic toxicity resulting in public health and environmental crises. Hence it is important to detect these residues in the food supply chain for food safety and public health. Metal–organic frameworks (MOFs) are a class of porous hybrid nanomaterials formed by networks of inorganic metal ions or metal clusters with mono-, bi-, and multi-dentate interlinked organic pliable electron-donating ligands and/or linkers. Owing to their atomic-level structural uniformity, tunable porosity, high surface area, flexibility in network topology, high density of active chemical sites, high chemical catalytic activity, *etc.*, these MOF-based nanomaterials can exhibit unique physical, chemical, and mechanical properties highly useful for sensing platforms. Developing

Received 23rd October 2022
Accepted 6th February 2023

DOI: 10.1039/d2fb00035k

rsc.li/susfoodtech

[a]*Department of Basic and Applied Sciences, National Institute of Food Technology Entrepreneurship and Management (NIFTEM), Haryana 131028, India. E-mail: physicsres.niftem@gmail.com*

[b]*National Horticulture Research and Development Foundation (NHRDF), Nashik-Aurangabad Road, Nashik, Maharashtra, 422003, India*

Mirinal Kumar Rayappa has completed his Bachelor of Technology (B.Tech) at the National Institute of Food Technology Entrepreneurship & Management (NIFTEM-K, INI Status), under the Ministry of Food Processing Industries, Govt of India. During this time, he was awarded the Indian Academy of Science Summer Research Fellowship at the Bhabha Atomic Research Centre, where he worked with Dr S. Jamdar and was a visiting research scholar at the Dr Marianne Ellis lab, University of Bath. Currently, he is pursuing Master of Research in Bioengineering at Imperial College London within the Güder research group. His wide research interests are multidisciplinary across the fields of biochemical analytical micro/nano-systems development, soft material chemistry and biomass valorization/processing.

Kavya K. S. has completed her Master of Technology (M.Tech) in Food Safety and Quality Management at the National Institute of Food Technology Entrepreneurship & Management (NIFTEM-K, INI Status), under the Ministry of Food Processing Industries, Govt of India. She is currently working as an analyst in central food testing facility in Bangalore after qualifying the junior analyst examination (JAE) conducted by the Food Safety and Standards Authority of India (FSSAI). Her research interests include food analytical chemistry and food quality studies.

nanomaterial-based sensors to identify and detect major antibiotic residues like beta-lactams, tetracyclines, macrolides, aminoglycosides, amphenicols, *etc.*, in consumer foods is of growing interest and MOF nanomaterial-based optical or electrochemical transduction sensors have been reported to show promising performance for antibiotic residue detection as an alternative to conventional techniques. Thus, this review presents the different classes of MOF-based nanomaterials and their synthesis, structure, functionalization, and sensing methodology to design a robust antibiotic residue detection sensor mainly useful in the food sector (including water). The discussions also extend to challenges and future research to be conducted to make these materials suitable for rapid testing of food samples along the food supply chain to establish a safer, secure, and sustainable food system.

1. Introduction

Antibiotics are commercially produced by modern biotechnology using metabolites derived from fungi and bacteria in natural fermentation, or chemically synthesised using synthetic substances. Antibiotics are a wide class of chemical compounds that can kill microorganisms or inhibit their growth. In veterinary medicine, antibiotics are therefore used as drugs for the treatment of diseases (such as mastitis, arthritis, respiratory diseases, gastrointestinal and various other bacterial infections). Hence there is a huge increase in the per capita consumption of these products over the years.[1] The over-the-limit administration of veterinary antibiotic doses to food animals to prevent diseases, for feed intake proficiency and growth enhancement, is one of the major reasons for antibiotic misuse.[2,3] Because of the potential toxic properties of antibiotic residues, the consumption of contaminated food with these residues establishes a direct risk for public health. Based on the Bayesian statistical model, it is estimated that the use of antibiotics in livestock will increase up to 200 235 tons by 2030.[4] Moreover, it is also possible that an estimated 30–90% of the administered antibiotics in food animals get excreted in the feces and urinal discharge due to their weak absorption in the animal's gut.[5] As a result, antibiotic residues have also been found in vegetables because of farmland soil pollution due to the use of antibiotic-containing untreated livestock excrements and wastewater as soil irrigation and manure.[6–8] Moreover, it has also been reported that these antibiotic residues, due to their high stability, are not destroyed even during the thermal processing of food products.[9] Details on the possible sources and routes of antibiotic residue presence in food supply chain systems have been elaborated by Chen *et al.*,[10] Table 1 shows various categories of veterinary antibiotic drugs and their examples used in animals from whom food prodcuts are derived for human consumption.

In a study carried out in Nepal, out of milk collected from three different sources (farmers, cottage dairies, and large dairy plants), 81% of samples showed residues of amoxicillin, 27% for penicillin, and 12% for ampicillin.[11] Penicillin-G residue was also detected in 41.1% fresh milk, 40.2% fermented milk, and 24.4% cheese.[12] Similarly in Bangladesh,

Dr Gurdeep Rattu completed his PhD (2022) in nanotechnology for the development of label-free optical chemical sensors for food safety & quality analysis at the National Institute of Food Technology Entrepreneurship & Management (NIFTEM-K, INI Status), under the Ministry of Food Processing Industries, Govt of India. Presently, he is working as a Senior Technical officer at the National Horticulture Research and Development Foundation, India (NHRDF). His wide research interests are in microbiology, bionanotechnology and molecular biology.

Dr P. Murali Krishna received his PhD (2008) in condensed matter physics from the Department of Physics, Andhra University, India. Currently, he is an assistant professor at the National Institute of Food Technology Entrepreneurship & Management (NIFTEM-K, INI Status), under the Ministry of Food Processing Industries, Govt of India. His lab research interests include the investigation of the chemical physics properties of materials and tuning them for various applications along with advanced instrumentation techniques. At present, his lab is developing nanomaterial-based label-free optical and electrochemical sensors for numerous onsite smart detection applications in agriculture, food, clinical, environmental, and green energy sectors, which are accredited by FSSAI and the Department of Biotechnology, Govt of India. He has more than 15 years of teaching and research experience with 34 published papers, 4 book chapters, 1 filed patent, and has won national fellowships.

Table 1 Various veterinary antibiotic classes and their examples used in various livestock and animal feed[2]

Antibiotic classes	Examples used in livestock
Aminoglycosides	Gentamicin, neomycin
Macrolides	Erythromycin, tilmicosin, lincomycin, tulathromycin, tylosin
β-lactams	Penicillin, ceftiofur, amoxicillin
Fluoroquinolones	Ciprofloxacin, danofloxacin, enrofloxacin
Tetracyclines	Chlortetracycline, oxytetracycline, tetracycline
Amphenicols	Chloramphenicol, florfenicol
Sulfonamides	Various sulfonamides
Nitrofurans	Nitrofurantoin

penicillin, tetracycline, and ciprofloxacin were found in both milk and eggs.[13] Oxytetracycline residues were also found in milk collected in Kerala, India.[14]

Epidemiological and toxicological studies have concluded that the ingestion of antibiotic residues can result in increased health risks for all age groups resulting in immunopathological effects, carcinogenicity, mutagenicity, nephropathy, hepatotoxicity, reproductive disorders, and even chronic toxic effects due to prolonged low-level exposure.[3,10] Apart from these ill effects, exposure to these residues will in-directly give rise to antibiotic-resistant bacteria with antibiotic-resistant genes that can cause greater harm to humankind.[15,16] This will also cause current antibiotic therapy to treat various diseases in humans to become a failure and the World Health Organization (WHO) has also declared it a global threat.[17,18] Also, the prevalence of these residues in the environment will enable environmental microbiome selection pressure (through horizontal transfer of antibiotic-resistant genes among microbes), thereby resulting in the creation of an antibiotic-resistant gene reservoir thus contributing towards a global environmental antibiotic-resistance to pathogens.[8] International bodies like WHO, the Food and Agriculture Organization of the United Nations (FAO), and the World Organization for Animal Health (OIE) are actively monitoring the timely scientific assessment of these antibiotic residues prevalence. In agreement with the WHO and CODEX, the Food Safety and Standards (FSSAI-India) issued mandatory regulations that all animal food products must be tested before their sales in the market. Furthermore, all the food business operators (FBOs) need to check for maximum permissible limits (MRLs) and should mention them on their food packaging labels. Table 2 summarizes the major antibiotic residues and their MRL in foods.

Conventional techniques like HPLC, ELISA, LC-MS, thin-layer chromatography (TLC), time-of-flight mass spectrometry (TOF-MS), microbial assay, capillary electrophoresis (CE), *etc.*, used for antibiotic residue quantification have issues such as being expensive per lab test, requiring a time-consuming procedure, trained personnel, central laboratory facilities, *etc.*[19] Biochemical sensors are seen as an alternative to these quantification methods since they are easy to handle, less expensive, portable, and rapid. These sensor are essentially a self-contained, integrated analytical tool that is used to quantify a target molecule of interest by making use of specific bio- or chemical receptors that are in proximity or are connected to a transduction system.[19] In this way, advanced nanomaterials have been used for the detection and quantification of low molecular weight organic and bio-macromolecular compounds and have eventually given rise to rapid, sensitive, portable, and on-site sensing choices.

Recently metal–organic framework (MOF) nanocomposites have gained interest in bio/chemical sensor development due to their specific properties and highly selective detection within and beyond the MRL detection ranges. MOFs make brilliant candidates for sensing applications due to many excellent features they offer such as controllable synthesis, reversible adsorption, high catalytic activity, tunable chemical functionalization, diverse structural constructability, large surface areas, high porosity, thermal stability, ability to be loaded with a high concentration of analytes and high compatibility with respective coordination elements.[20–22] A wide range of linkers can be incorporated into MOFs and multiple metals can also be used to synthesize MOF structures. MOFs have a large surface area that is comparable to that of zeolites with multi-size pore structures, which helps in easier capture of analytes during analysis. Post-synthesis modification can also be carried out to change the physical and chemical properties of MOFs.[23] MOF-based sensors are less harmful to the environment as they use far fewer hazardous chemicals compared to chromatographic techniques. Hence, there is growing research interest in the development of MOF nanomaterial-based sensors to detect different analytes such as environmental pollutants, antibiotics, VOCs, heavy metals, and other gaseous compounds.[24]

Despite many papers that have focused on antibiotic detection using various materials, a focused review on MOFs as nanomaterials for antibiotic residue detection in food (including water) with recent advancements is timely and of need. Xenobiotic agents (synthetic chemical substances that are not naturally present in an organism) such as these antibiotic residues are contaminants that are inherently not present in food and are vertically and horizontally transferred across the agro-food chain starting from livestock and agro sources to the natural environment and human consumption products. Such prevalence requires routine monitoring by chemically testing food samples at critical control points (such as testing the food products right before packaging them for retail at food establishments or at a mobile laboratory facility utilizing portable systems for facile testing across livestock farmlands) before sending them across the market for direct human purchase and consumption. Such testing

Table 2 MRLs for antibiotic residues in various foods (based on FSSAI and CODEX guidelines)

Antibiotics	Foods	FSSAI MRL (mg kg^{-1})	CODEX AND FAO MRL (mg kg^{-1})
Amoxicillin	Milk	—	0.0004
	All other tissues	—	0.005
Ampicillin	All foods	0.01	0.005
Streptomycin	Muscle	0.6	—
	Liver	0.6	—
	Kidney	1	—
	Fat	0.6	—
	Milk	0.2	—
Tetracyclines	Muscles	0.2	0.2
	Liver	0.6	0.6
	Kidney	1.2	1.2
	Milk	0.1	0.1
	Eggs	0.4	0.4
	Honey	0.005	
Erythromycin	Muscles	0.1	0.1
	Liver	0.1	0.1
	Kidney	0.1	0.1
	Fats	0.1	0.1
	Eggs	0.05	0.05
Sulfonamides	All foods	0.01	0.1
	Milk	—	0.025
Chloramphenicol	All food	0.0003	Should not be permitted
Nitrofurans	All foods	0.0001	Should not be permitted

will result in rejecting raw materials right before they are extensively distributed across the supply chain thereby establishing risk-based monitoring with flexible sampling. Therefore, as opposed to conventional high-end central laboratory instruments that are known to identify accurate levels of these residues in food, the alternative material must possess such relative properties to detect the same at least at the lowest levels far below the MRL if not at exact trace level-fingerprinting. With such views, this paper presents a brief narrative of the current scenario of commonly present veterinary antibiotic residues in food followed by a discussion on novel MOF nanomaterial synthesis, their structures, surface modification, and their sensing of these residues by means of optical and electrochemical detection mechanisms in food samples. Further discussions about impediments to using MOFs, and their improvements for antibiotic residue detection in animal-derived food and an emphasis on plant-derived food have also been presented for routine chemical analysis of these residues. Fig. 1 gives an overview of sensing applications in a food chain for detecting veterinary antibiotic residues.

2. MOF synthesis, structure, design, and class

Metal–organic frameworks (MOFs) are a class of nanoporous, coordination networks of polymeric hybrid crystalline materials that are composed of inorganic metal ions or metal clusters that are interlinked or connected *via* pliable electron-donating organic ligands or linkers using strong covalent bonding.[22,25,26] The pore size of the MOFs is well defined with a high specific surface area (beyond a Langmuir surface area of 10 000 m^2 g^{-1}) which is several times higher than that of activated carbon (1200 m^2 g^{-1}) and can also be tuned to desired sizes (from angstroms to nanometers) as per specific functional application.[21] In this way, highly porous and structurally diverse MOFs can be constructed using hybrid and synergistic composite materials with various functional sites and tunable physicochemical properties to achieve specific molecular recognition activity in sensing applications. MOFs can be custom fabricated or tailored into the desired dimension (1D, 2D, or 3D) and geometries (linear, trigonal, tetrahedral, square planar, octahedral, and various pyramidal types) to suit analytical detection by making the conscious selection of the metal ion and the organic linker to form a good network of repeating coordination entities.[25] MOFs have been successfully fabricated using various polymers, metal-oxide nanoparticles, quantum dots, graphene, carbon nanotubes, biomolecules, and even laudable integration with various functional materials as well.[26] This paved the path for multifunctional composites to be integrated into a controlled and coordinated fashion to form novel MOFs with superior, collective, and synergistic properties apt for a wide or narrow range of applications. The three different methods used for modifying and functionalizing MOFs include:

- Modification of specific organic ligands or doping of metal ions into the frame of MOFs.[23,27]
- Post-synthesis modification, in which the organic linkers with functional groups can be used for subsequent chemical grafting.[27,28]
- Entrapment of functional molecules and nanoparticles (NPs) within the framework, so that the resulting composites

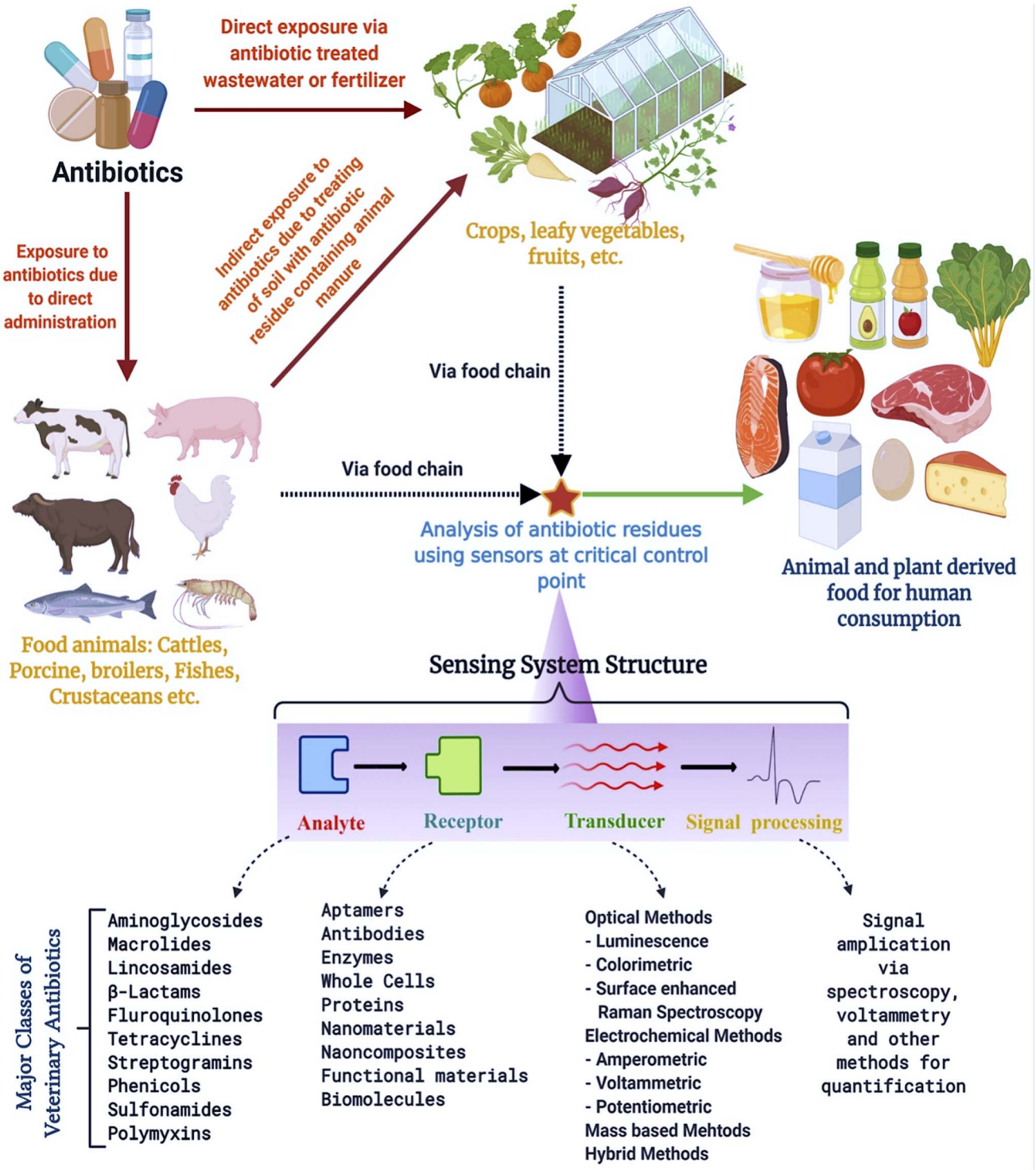

Fig. 1 Sources of antibiotic residues in foods and their detection using sensors at critical control points within a food chain.

come to possess multiple functionalities for molecular recognition and signal transduction.[27]

Many methods including sonochemical, solvothermal, microwave, hydrothermal, and microemulsion methods have been employed in the synthesis of MOF nanoparticles. The most common is the solvothermal method that produces MOFs with a particle size between 300 and 800 nm. It is effective in synthesizing MOFs of varying sizes, as well as controlling the size with control modulators. Therefore, the addition of various modulators of varying concentrations affects the size of the resulting MOF. Xia *et al.* synthesized ZIF-67 crystals of varying sizes using different solvents (modulators) such as ethanol (bulk), deionized water, and methanol under conditions of 120 °C (3 days) and 60 °C (20 h) respectively.[29] Rapid synthesis and

nucleation can be accomplished through microwave synthesis. This in turn can help in size reduction. A 104 nm size nano-cubic crystal was synthesized with the microwave method in less than 2 minutes.[30] Microemulsion can also facilitate rapid synthesis and effective size reduction. MOFs in quantum dot structures (less than 2 nm) have also been able to be synthesized.[31] Rapid kinetics, nucleation, and phase control are also possible in the sonochemical approach. The ultrasonic wave increases the temperature and pressure of the solution through the growth and collapse of the acoustic cavity. Li *et al.* synthesized MOF NPs of 200–400 nm using a sonochemical approach.[32]

Nanorods, nanowires, and nanotubes are 1-dimensional structures that are synthesized by controlled synthesis using polycarbonate membranes *e.g.* ZIF-8. More research can be conducted to utilize these 1-D structures for antibiotic detection, which is very scarce.[33,34] While many nanosheet and nanofilm structured MOF attempts have been conducted for the synthesis of 2D MOFs, most reports exist for wide 3D geometric MOF sensor development for antibiotic residue detection.[35] Of these, porous MOFs have been shown to be very apt for the absorption and detection of antibiotic residues in food[36] based on a variety of network modifications in both 2D and 3D models with high porosity, high ion exchange, and adsorptive properties. This high level of properties could be achieved by intermolecular interactions and metal–ligand coordination.

In contrast to existing materials such as metal oxides, others like porous metal membranes, nanostructured thin films, and conducting polymer MOFs have a high surface area, which provides a large concentration of chemical recognition active sites. Although high porosity can enhance the above-mentioned properties, MOFs still have strong nonspecific adsorption forces that retain other small molecules under ambient conditions due to their porosity. This limitation can be overcome with MOF surface modifications and the incorporation of hybrid materials into molecule binding sites typically as shown in Fig. 2. This will allow for feasible hybrid MOF processability, band gap engineering, and sensing property tailoring, thus making these MOF materials promising candidates in the construction of electrochemical, optical, and other sensors.

The thermodynamics and kinetics of MOF structures differ with various metals and ligands used and also differ with each framework design. The relative rate of diffusion of precursors in the solution is fast compared to the formation of metal–organic ligand coordination bonds.[38] MOFs are constructed by tailoring inorganic polynuclear metal clusters known as secondary building units (SBUs) and organic linkers *via* strong bonds that may show a controlled period of homogenous nucleation in complex phase reactions with the chance for good particle size tuning during the growth of these NPs.[39,40] SBUs are the key components of MOFs that help to build potentially porous periodic networks by linking multitopic organic ligands and play an important role in the absorption properties of MOFs.[41–43] Most MOF NPs are synthesized by any of the following methods, or sometimes in combination: (1) rapid nucleation, (2) nanoreactor confinement, and (3) coordination modulation.[44] The various mechanisms involved in the controlled synthesis of MOF NPs are shown in Fig. 3(a–c). The Lamer model of nanoparticle growth was mainly used for understanding the mechanism of MOF NP nucleation and growth as shown in Fig. 3(c). In the Lamer model,[44] the process of nucleation and growth takes place in four steps:

(1) A swift rise in the number of reactive monomers in solution (stage I).

(2) A uniform nucleation "burst" as the number of reactive monomers surpasses the critical nucleation concentration (C_{nuc}).

(3) A swift reduction in the number of monomers in the solution, thus stopping the further nucleation process (stage II).

(4) And an increase in crystal growth when the saturation concentration is reached (C_{sat}) (stage III).

To synthesize small, uniform-sized MOF NPs, many nuclei need to be produced through nuclei burst nucleation followed by

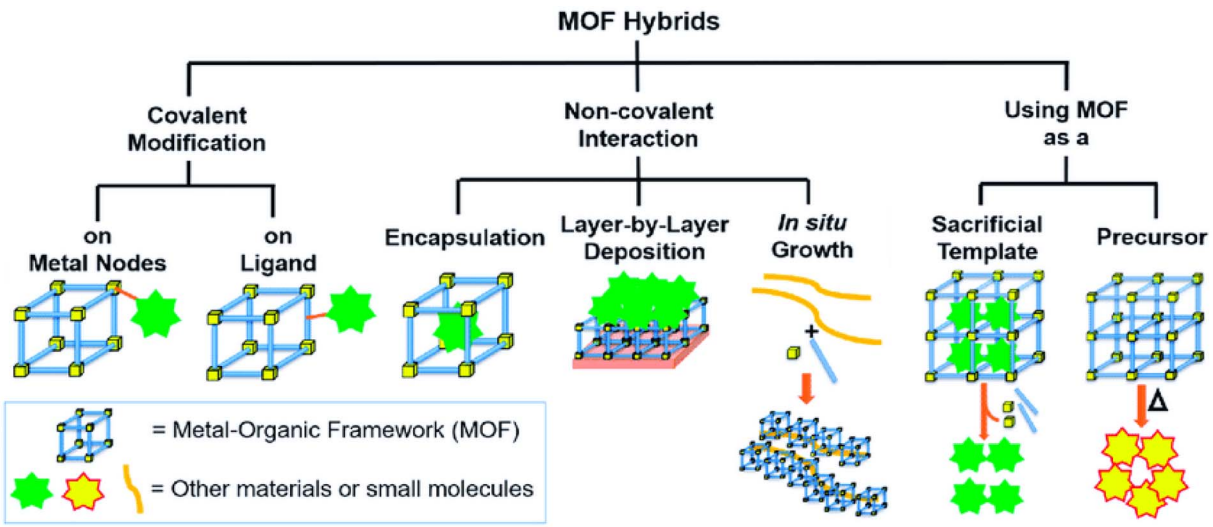

Fig. 2 Metal organic framework hybrid synthesis *via* various modfication methods. Reproduced with permission from mdpi.[37]

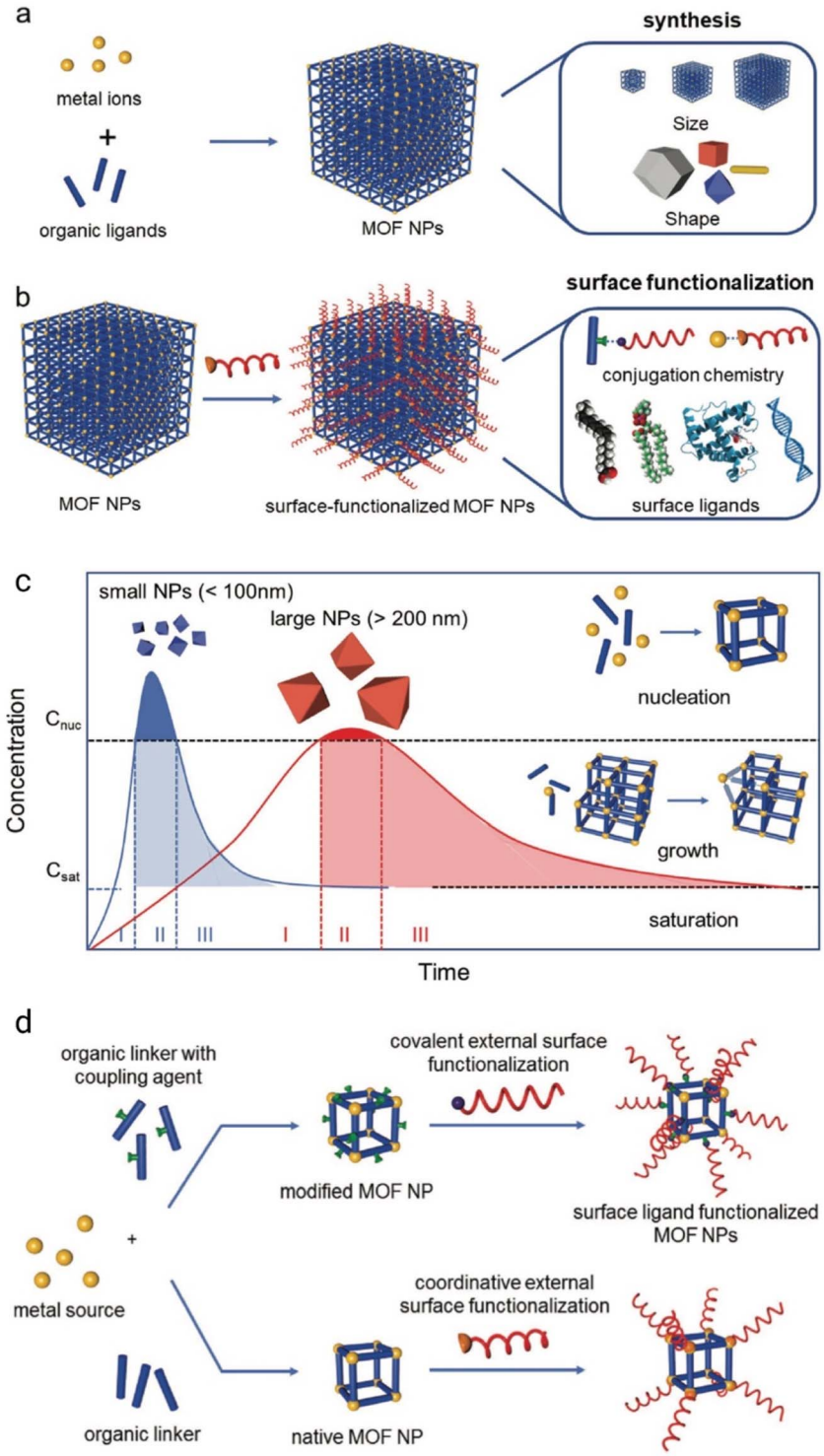

Fig. 3 Schematic diagram of (a) the controlled synthesis of MOF NPs, (b) the post-synthetic surface modification of the MOF, (c) lamer model of four steps of MOF NP formation, and (d) covalent surface modification (top) and coordinative surface modification (bottom) at the SBUs. Reproduced with permission from Wiley.[44]

rapid depletion of precursors to avoid further particle growth. Large MOF NPs are obtained by slow particle nucleation and growth. The standard techniques like X-ray absorption of fine structures,[41] high-resolution TEM,[42] liquid cell transmission electron microscopy (LCTEM),[40] time-resolved static light scattering,[43] small- and wide-angle X-ray scattering,[38] *etc.* have been performed to find the structural, morphological and porosity characteristics during this nucleation and subsequent MOF fabrication.

3. Surface functionalization of metal–organic frameworks for sensor development

To improve the performance of the MOF sensing mechanism, the necessary functional groups will be grafted to MOFs and the length of the metal–oxygen bond also plays a key role in activating the reactants. Generally, the desired functional group introduction in the post-synthetic approach is more advantageous than the direct synthetic approach. Post-synthetic modification of MOFs facilitates the incorporation of functional groups into MOF structures without damaging the basic framework structure. The metal ions or the clusters, through the linker

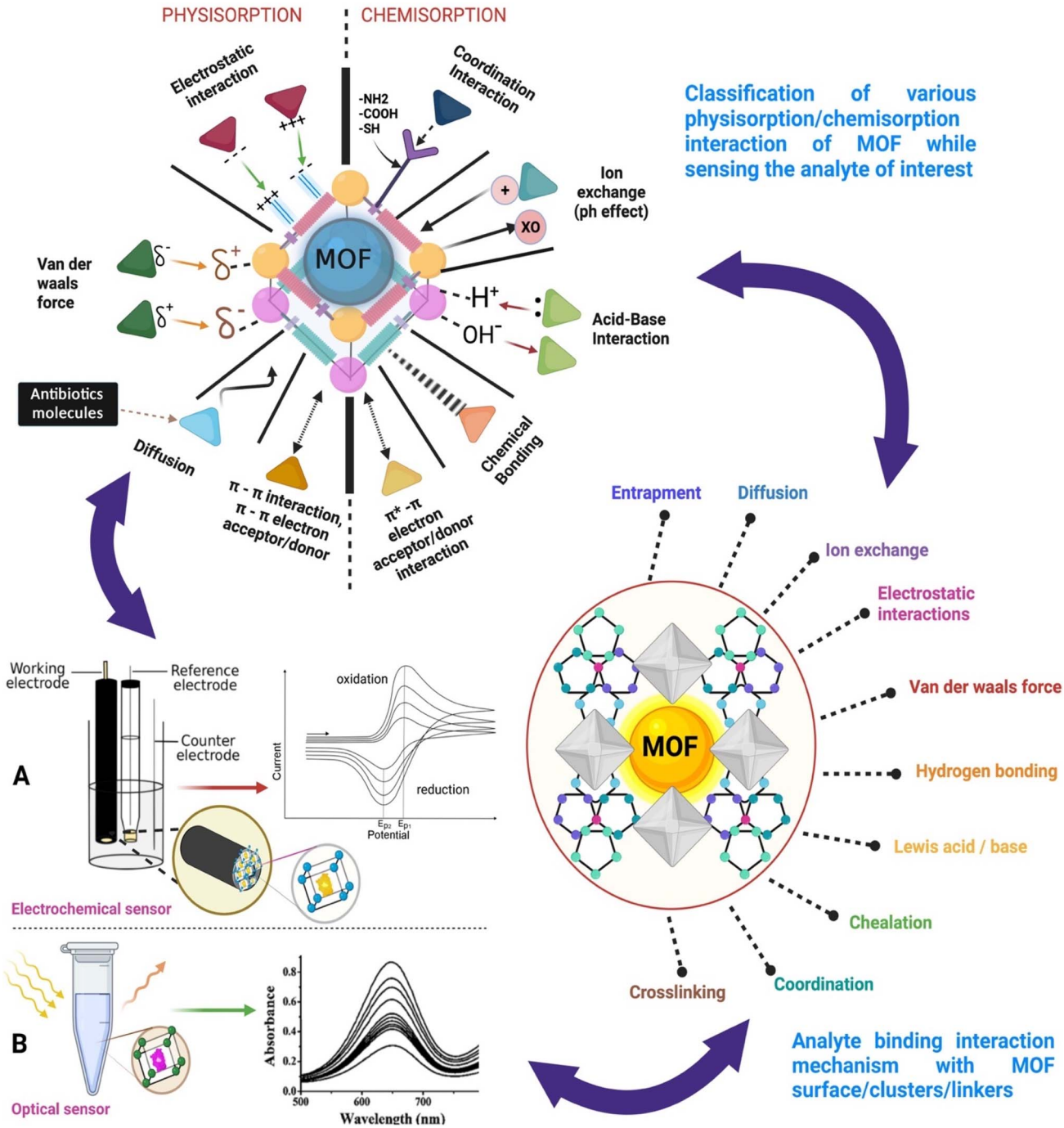

Fig. 4 Typical physic–chemical kinetics of analyte (antibiotic) molecular functional group interaction with surface functionalized MOFs in selective detection and for optical and electrochemical bio/chemical sensor designing. Commonly used transduction methods for sensing such as (A) an electrochemical sensor having a MOF based working electode with subseuqnt analyte responsive redox signal and (B) an optical sensor containing MOF based reagent with a subsequent analyte concentration based spectrocopic signal. Modified from ref. 58 and 59.

strategy, allow for various molecule groups such as hydroxyl, thiol, or amide and even biomolecules such as aptamers to be functionalized as selective binding/interaction sites through different physisorption and chemisorption interactions. A schematic illustration of the interactions/mechanisms involved in the adsorption of analytes (antibiotic residue in this work) to the metal–organic frameworks (MOFs) and their optical and electrochemical transduction is shown in Fig. 4(A and B). The stability, solubility, catalysis, and sensing properties are all modulated by surface ligands. Some of these properties might turn out favourable for specific purposes and others may not so too. Therefore, post-synthetic modification (PSM) of the external surface of MOF NPs is necessary to induce desired effects such as increase in colloidal stability, stimuli–responsive reactions, and bio/chemical marker targeting.[45,46] Most of the time organic molecules like nucleic acid, lipids, peptides, and some polymers are used as surface ligands due to their chemical flexibility and the steric effect that does not allow them to diffuse into pores. There are two types of surface functionalization commonly used namely (1) covalent surface functionalization and (2) coordinative surface functionalization[44]

3.1 Covalent surface functionalization

Covalent surface modification is based on the placement of highly reactive functional groups such as amine, carboxylic acid, and azide on the organic linker moiety of a MOF before the synthesis of the actual MOF. This is a robust way of modifying MOF NPs without obstructing nanoparticle formation. This is usually a complex and tedious process. These functional groups then are allowed to react with the carbonyl, amine, or alkynes group present in the modifying surface ligands in post-synthetic functionalization. Polymers and biomacromolecules such as lipids, proteins, nucleic acids, and some sugars (oligosaccharides) are some of the best options to be used as surface ligands. Covalent post-synthetic functionalization can lead to a low density of surface modification, dissociation, or association of surface ligands with other molecules leading to unstable MOF structures and reduced porosity.[44]

3.2 Coordinative surface functionalization

In coordinative surface functionalization, rather than modifying the organic linker molecule in the MOF to attach to the surface of the ligands, the metal moiety of the MOF is utilized. The metal atoms are capable of forming coordinate bonds using electrons in the d-orbitals. The metal atom acts as the electron donor and the surface ligands act as the acceptor, thus forming a coordinate bond. This is an uncomplicated synthesis without using reagents or other linkers and the MOF very well retains all its desirable properties.[44]

To achieve good sensing properties and methodologies, it might be necessary to apply more than one surface binding mechanisms to enhance the selectivity, adsorptive capability, and transduction mechanism of the sensor.[58] This can be achieved by surface functionalization strategies of different types of metal, clusters, or core–shell MOFs through molecule linkers type (typical groups such as hydroxyl, thiol, or amide, biomolecule, aptamers, *etc.*) which will function as active binding/interaction sites using various physisorption and chemisorption interactions with the analyte as given in Table 3 and Fig. 4.

4. MOF based optical sensors

MOF optical properties often arise from the linker molecule as many of these conjugated linkers exhibit fluorescence and/or absorb light in the UV-visible range. While many of the studied MOFs typically contain d^{10} metal ions which do not exhibit light-emitting electronic transitions, f-element metal centres (*e.g.* lanthanide and actinide metals) have also been used as luminescent MOF sensors. Highly absorbing conjugated linkers can amplify the emission throughout the extended network as energy is transferred from node to node among these luminescent MOF structures further enhancing their sensing ability. Luminescence sensing with MOFs can be achieved through the enhancement, quenching, or shifting of fluorescence signals upon target adsorption. The extended π-conjugation and interlayer π–π interaction in the nanosheet morphology of MOF structures have been extensively utilized to promote fluorescent emission in sensing.

In addition to *de novo* design, tuning by the post-synthetic modification of the pore interior and/or the inclusion of fluorophores as guest molecules into the pores, such as lanthanide ions, quantum dots (QDs), fluorescence dyes, *via* coordination or covalent bond formation within the backbone of MOFs is often exploited for optical sensing. The phenomenon of increasing the absorption or emission intensity that represents higher energy absorption and conversion efficiency, *i.e.*, a shift in the emission wavelength across a wider range of wavelengths, offers a good candidate for fluorescence-related MOF applications. With various sensing mechanisms explored using MOFs for antibiotic residue detection, a comprehensive compilation of such recent MOF nanomaterials, their sensing mechanism (optical and electrochemical), linear range, and LOD studied for food and water antibiotic residues is presented in Table 4.

4.1. Fluorescence/luminescence sensor

In an optical sensor, changes in light transmission, reflection, refraction, absorption, amplitude, phase, frequency, or polarization occurring during bio/chemical recognition events are taken to be proportional to the concentration of the target analyte being measured in a sample.[60] Most of the MOF-based sensors developed for antibiotic residue detection in food mainly use optical-based transduction systems. Of these, most of the optical sensors are based on fluorescence (FL) or luminescence (LU) quenching (since all of them consist of a lanthanide or an aromatic fluorophore) and use various sensing mechanisms such as photo-electron transfer (PET), intermolecular charge transfer, resonant energy transfer (FRET) and competitive adsorption.[27,61] A MOF sensor is synthesized in such a way that the emission spectra of the MOF align exactly with the absorption spectra of antibiotic residues so that when MOF emission occurs in the presence of antibiotic molecules,

Table 3 Summary of surface functionalization strategies. Adapted from ref. 47

Type of strategy	Strategy	Typical surfactants/molecules	Ref.
Replacement	Ligand exchange	Ligands with a chemical group that binds the NP (thiols, amines, phosphines, carboxylic acids), micelle structure, contains a polar head group (hydroxyl) on the other end, *etc.* Bidentate ligands Linear and branched polymers	48
	Ligand addition	Similar ligands as used in ligand exchange ones	49
Noncovalent conjugation	Bilayers	Alkyl carboxylic acids, phospholipids	50
	Wrapping	Large-molecular-weight polymers	51
	Encapsulation	Amphiphilic polymers: the hydrophobic groups interact with the surface-bound ligand and hydrophilic groups provide water solubility	52
	Electrostatic conjugation	Highly charged polymers made up of molecular entities with multiple charges	53 and 54
	Metal affinity coordination	NPs with metals on the surface such as Fe^{2+}, Ni^{2+}, Zn^{2+}, or Cu^{2+} Electron donor molecules such as polyhistidine	53 and 55
	Host–guest interaction	Coupled moieties like cyclodextrin and adamantyl moieties	56
Covalent conjugation	Sulfur bridged	Thiol-terminated molecules	57
	Click chemistry	Azido-terminated molecules: this allows the crafting of the polymers on the surface of the NPs	53
	Carbodiimide chemistry	Usually for NPs with carboxyl groups on the surface, amine-terminated molecules, amino acids, peptides, and proteins	53

a decrease in the fluorescence occurs. There are mainly four reasons for this FL/LU quenching such as (1) collapse of the MOF structure, (2) photoinduced electron transfer, (3) resonance energy transfer and (4) inner filter effect.

Since most sensors use stable MOF structures to detect their corresponding analyte, the collapse of these structures can be ruled out as a reason for the fluorescence quenching. Hence the quenching is mainly due to either one or more of the other reasons mentioned above. The photoinduced electron transfer (PET) is a redox reaction in which excited electrons are transferred from the donor to the acceptor in the presence of light. *i.e.*, one species gets oxidized while the other is reduced. The electron transfer between the metal and the ligand in the HOMO (Highest Occupied Molecular Orbital) and LUMO (Lowest Unoccupied Molecular Orbital) energy levels causes fluorescence/luminescence. Most antibiotic molecules contain furan or benzene rings that can act as electron donors or acceptors respectively. Hence the interaction between the MOF and various antibiotics compounds brings about a quenching of fluorescence/luminescence. The other mechanism is due to the transfer of energy in either direction between light-sensitive molecules *i.e.*, the analyte and the fluorophore. An excited state fluorophore transfers its energy to a ground-state fluorophore through nonradiative dipole–dipole interaction. This interaction is distance dependent and once again exploited by functionalizing MOFs with such fluorophores. The overlap between the absorption spectra of the analyte and the emission spectra of MOF causes quenching, *i.e.*, in both PET and FRET, during the detection of these antibiotic residues, and the emission spectra of MOF are absorbed by the analytes, which decrease the intensity of fluorescence, which can consequently be quantified by using a simple fluorometer. This decrease in the intensity is proportional to the concentration of the analyte. In some sensors, the shift of spectra or enhancement of fluorescence can also occur due to the formation of new complexes.[36,62] The inner filter effect can also be a reason for the fluorescence quenching. The ligands absorb energy from a light photon and simultaneously transfer this energy to the transition or lanthanide-type metal ion by the "antenna effect". The overlapping of the absorption spectra of antibiotics and the excitation spectra of the MOFs blocks the "antenna effect" in transition or lanthanide MOFs due to the filter effect that may act internally in the MOF's sites binding mechanism.

Table 4 Summary of sensor types, MOF- nanomaterial used, the food sample studied with a particular antibiotic residue as the analyte, the recognition mechanics used, and the respective linear range and limit of detection reported are arranged in descending order of research and development over the years[a]

Sensor type	MOF	Sample	Analyte	Mechanism	Linear range	Lod	Reference
Optical based							
Electrochemiluminescence	Gold incorporated HKUST with a cysteine perylene derivative	Milk	Kanamycin	In the presence of analyte, the catalytic activity of the MOF increases the binding of the aptamer–analyte complex resulting in increased luminescence intensity	1.0×10^{-13} to 1.0×10^{-8} M	20.34 pg L^{-1}	85
Fluorescence	Eu MOF	Water	Metronidazole, dimetridazole	Fluorescence quenching due to PET and FRET mechanisms	—	13 μg L^{-1}, 13.4 μg L^{-1}	86
Fluorescence	Eu MOF	Milk, beef	Tetracycline	Inner filter effect and PET	—	19.1 μg L^{-1}	87
Ratiometric fluorescence	Zeolitic imidazolate framework-8 incorporated with a gold cluster and green-emitting carbon dots	Milk	Cephalexin	The gold cluster has an emission wavelength of 630 nm and green-emitting carbon dots have an emission of 520 nm when excited at 400 nm. Cephalexin selectively quenches the emission of the gold cluster while the fluorescence of carbon dots remains the same. It can be noted that the ratio of emission (F_{520}/F_{630}) is linearly proportional to the concentration of the analyte	0.1-6ng L^{-1}	0.04 ng L^{-1}	88
Fluorescence	MIP-coated Zr MOF	Honey, milk	Chloramphenicol	The non-homogeneous adsorption of the analyte on the surface of the MOF enhances the fluorescence emission	0.16–161.56 μg L^{-1}	0.013 μg L^{-1}	89
Luminescence	Al MOF	Milk	Nitrofurazone, nitrofurantoin, furazolidone	Spectral overlap of absorption spectra of the analyte and excitation spectra of the MOF	—	105 μg L^{-1}, 200 μg L^{-1}, 131 μg L^{-1}	90
Fluorescence	Tb MOF	Milk	Tetracycline	Inner filter effect and FRET	0–244 μM L^{-1}	88.5 μg L^{-1}	91
Fluorescence	Eu MOF	Aqueous media	Ciprofloxacin, ofloxacin	Fluorescence quenching due to PET and dynamic fluorescence quenching mechanisms	—	0.693 ng L^{-1}, 0.802 ng L^{-1}	92
Fluorescence	Tb^{3+} doped Zn MOF	Aqueous media	Nitrofurazone	Inner filter effect and FRET	0–3.4 μM	115 μg L^{-1}	93
Fluorescence	Eu MOF and Tb MOF	Aqueous media	Cefixime, nitrofurazone	At lower concentrations, competitive absorption of the excitation wavelength by the analyte and higher concentration electron transfer between the analyte and MOF	0–0.05 μM	$Eu_{(cefi)}$ 1.8 mg L^{-1}, $Tb_{(cefi)}$ 1.9 mg L^{-1}, $Eu_{(nitro)}$ 1.8 mg L^{-1}, $Tb_{(nitro)}$ 1.6 mg L^{-1}	94

Table 4 (*Contd.*)

Sensor type	MOF	Sample	Analyte	Mechanism	Linear range	Lod	Reference
Fluorescence	Lanthanide doped Zr and Zn MOF	Milk	Norfloxacin, minocycline	Fluorescence enhancement by the energy transfer from the analyte to the MOF is the detection mechanism in norfloxacin and fluorescence quenching due to the inner filter effect and a possible complex formation in the case of minocycline	2–200 μM for minocycline, 0.4–20 μM for norfloxacin	5.6 mg L^{-1} for minocycline, 19.1 μg L^{-1} for norfloxacin	95
Fluorescence	Tb MOF	Aqueous media	Nitrofurans, nitroimidazoles, sulfamethoxazole	The nitro group containing antibiotics acts as an electron acceptor and the ligands as the electron donors causing fluorescence quenching, but sulfamethoxazole has a higher LUMO than the ligand and therefore acts as an electron donor and causes fluorescence enhancement. The I_{544}/I_{400} value increases in the case of nitrofurans as the concentration increases whereas the value decreases in the case of the concentration of nitroimidazoles	—	98 μg L^{-1} and 196 μg L^{-1} respectively for nitrofurantoin and dimetridazole	96
Fluorescence	(Zn-MOF), $[Zn_2(oba)_4(4,4'\text{-bpy})_2]_n$	Aqueous solution	Metronidazole	The absorption spectra of met antibiotic overlap with the fluorescence spectra of Zn-MOF causing fluorescence quenching	0–400 μM L^{-1}	0.81 mg L^{-1}	67
Fluorescence	$\{$(Cd-MOF) $[Cd_2(HL)_2(bip)_2]\cdot H_2O\}_n$	Aqueous solution	Chloramphenicol	Fluorescence quenching – the PET process (photoinduced electron transfer) in H_3L and antibiotics	0–10 μM L^{-1}	91 mg L^{-1}	97
Luminescence	Cd-MOF $[Cd_4(L)_4\cdot H_2O\cdot EtOH]_n$	Water	Nitrofurantoin	The overlap between the UV-Vis adsorption band of NFT and the emission of MOF-luminescent quenching	—	2.4 mg L^{-1}	98
Fluorescence	$[Cd_2(HDDB)(bimpy)(NMP)(H_2O)]$	Water	Nitrofuran/nitroimidazole (1,2-dimethyl-5-nitroimidazole; metronidazole; ronidazole; ornidazole and two nitrofuran antibiotics (nitrofurazone, nitrofurantoin)	Fluorescence quenching by PET (photoinduced electron transfer) and FRET (fluorescence resonance energy transfer)	0–0.5 mM L^{-1}	52 μg L^{-1} for DND, 80 μg L^{-1} for MND, 102 μg L^{-1} for RND, 81 μg L^{-1} for OND, 136.7 μg L^{-1} for NFZ and 2.62 mg L^{-1} for NFT	65
Fluorescence	$[Cd_2Cl(L)(H_2O)]\cdot 11H_2O$	Water	Nitrofuran (nitrofurazone and nitrofurantoin)	Fluorescence quenching by photoinduced electron transfer (PET)	10^{-6} to 10^{-3} M L^{-1}	40 μg L^{-1} for NFZ and 61 μg L^{-1}NFT	63

Table 4 (*Contd.*)

Sensor type	MOF	Sample	Analyte	Mechanism	Linear range	Lod	Reference
Colourimetric sensor	Aptamer (Apt)-capped and horseradish peroxidase (HRP)-embedded zeolitic metal azolate framework-7 (MAF-7) (apt/HRP@MAF-7)	Milk and water	Streptomycin	The aptamer interaction with the streptomycin triggers the enzymatic (HRP) catalysis of TMB in the presence of H_2O_2	0.005–6 ng mL^{-1}	0.51 pg mL^{-1}	74
Fluorescence	Ln MOF, Ln = Tb^{3+}	Water	Oxytetracycline, tetracycline	The absorption spectra of OTC and TCT align with the emission spectra of Ln MOF strips causing fluorescence quenching	0–0.05 mM L^{-1}	0.96 μg L^{-1}, 1.3 μg L^{-1} for OTC & TCT	70
Fluorescence	Zeolite imidazolate framework-8 (ZIF-8) is anchored on a two-dimensional (2D) amino-functionalized Al-metal organic framework (NH_2-MIL-53(Al))	Milk	Doxycycline, tetracycline, oxytetracycline and chlortetracycline	The overlap of the absorption spectra of TCs with the fluorescence excitation spectrum of ZIF-8/NH_2-MIL-53(Al) illustrates that the inner filter effect (IFE) contributes to the fluorescence quenching	0.004–38.5 mg L^{-1} for TCT, 0.004–25.7 mg L^{-1} for DOX, 0.004–32.1 mg L^{-1} for OTC, 0.005–25.7 mg L^{-1} for CTC	1.2 μg L^{-1} for TCT, DOX, and OTC and 2.2 μg L^{-1} for CTC	66
Fluorescence	Phosphate and fluorescent dye 6-carboxy-*x*-rhodamine (ROX) double-labelled aptamers of CMP and the bimetallic organic framework nanomaterial Cu/UiO-66	Fish	Chloramphenicol	The fluorescence of ROX dye in the absence of CMP antibiotic is quenched by the PET. In the presence of CMP, there is a change in the spatial arrangement of the particle causing the regaining of fluorescence	0.2–10 nM L^{-1}	29 ng L^{-1}	68
Luminescence	Ln-MOFs {$[H_3O]$-$[Ln_5(L)_4(DMA)_2]\cdot 4.5H_2O$}n (Ln = Eu^{3+} (1) or Tb^{3+} (2))	Aqueous medium	Ornidazole	The reduced luminescence intensity is caused by the adsorption of OND in the UV-vis region as well as the collision interaction between MOF structures and free OND that consumes emitted light energy	490–510 μg L^{-1}	2 μg mL^{-1}	71
Fluorescence	Al MOF@Mo/Zn-MOF heterostructure	Aqueous medium	Doxycycline, tetracycline, oxytetracycline and chlortetracycline	The intense absorption of TCs hinders the excitation energy absorption of the Al-MOF@Mo/Zn-MOF nanoprobe, which results in remarkable FL quenching due to the relevant inner filter effect (IFE)	DOX – 0.001–53.33 μM L^{-1}, TCT, OTC and CTC 0.001–46.67 μM L^{-1}	0.25, 0.25, 0.28 and 0.44 μg L^{-1} for DOX, TCT, OTC and CTC	64
Fluorescence	Europium MOF-Eu-In-BTEC	Fish	Doxycycline	The unique interaction between europium and doxycycline forms a complex which has a dual-channel fluorescence which increases the total emission	0–6 μM L^{-1}	21 μg L^{-1}	99
Colourimetric	Gold nanoparticle-aptamer combined with iron-MOF (Fe-MIL-53)	Water	Chloramphenicol	The AuNP–aptamer interaction with antibiotic decreases nanozyme (FeO_3 MNP) catalysis of TMB in the presence of H_2O_2	50–200 nM L^{-1}	8.1 ng mL^{-1}	73

Table 4 (*Contd.*)

Sensor type	MOF	Sample	Analyte	Mechanism	Linear range	Lod	Reference
Fluorescence	Nanoscale luminescent MOF In-sbdc	Milk, fish, pork	Tetracycline	The large overlap between the absorption spectrum of tetracyclines and the emission spectrum of the MOF causes fluorescence quenching	0–30 μM L^{-1}	135 μg L^{-1}	100
Fluorescence	Dye dopped UiO66 MOF	Milk, honey	Tetracycline	The MOF has a characteristic blue emission (430 nm) due to the dye. But in the presence of TCT, there is red emission (617 nm) from the incorporated Eu^{3+} ion – TCT complex due to the antenna effect. The blue emission from the dye remains unchanged and hence can be a reference	0.1–6 μM L^{-1}	8.61 μg L^{-1}	72
Luminescence	Luminescent MOF $[Zn_8(C_5H_4N_5)_4(C_{14}H_8O_4)6O(C_{50}H_{44}N_4)_{0.5}]$(TMPyPE@bio-MOF	Aqueous medium	Nitrofurazone, nitrofurantoin	The strong adsorption of NFZ and NFT near the excitation wavelength of the MOF suppresses the excitation energy absorption of TMPyPE@bio-MOF-1, causing fluorescence quenching	—	0.110 μg L^{-1} for NFZ 0.134 μg L^{-1} for NFT	101
Luminescence	Zinc-based metal–organic framework of pyromellitic acid (Zn-BTEC)	Fish	Chlortetracycline	The aggregation of the rigid MOF–CTC complex enhances the fluorescence of the media	0–8 μM L^{-1}	14.4 μg L^{-1}	102
Luminescence	Luminescent metal–organic framework (LMOF) $[Zn_4O(BCTPE)_3]$	Water	Nitrofurazone, metronidazole	Excited-state electron transfer from the higher LUMO of H_2BCTPE to those of the analyte may occur under photon excitation (PET), resulting in severe fluorescence quenching	—	0.1 μg L^{-1}, 0.6 μg L^{-1}	69
Fluorescence	Cu MOF based aptasensor	Milk, fish	Chloramphenicol	The main mechanism is FRET. The aptamer hairpin probe in the sensor along with SYBR green dye, in the absence of CMP, gets adsorbed on the Cu MOF and its fluorescence is quenched. In the presence of CAP, the aptamer forms a ds-DNA with the primer, and its fluorescence is enhanced, and this dsDNA is not adsorbed on the Cu MOF	0.001–10 ng L^{-1}	0.3 pg L^{-1}	103

Table 4 (*Contd.*)

Sensor type	MOF	Sample	Analyte	Mechanism	Linear range	Lod	Reference
Chemiluminescent	Luminescent heterometallic MOF, $[NaEu_2(TATAB)_2(DMF)_3]\cdot OH$ (CTGU-7, H_3TATAB = 4,4′,4″-*s*-triazine-1,3,5-triyltri-*m*-aminobenzoic acid, DMF = *N*,*N*′-dimethylformamide, CTGU = China Three Gorges University)		Ornidazole	The luminescence quenching is caused by the energy transfer between the compounds	—	0.18 mg L^{-1}	104
Electrochemical sensors							
Impedance	Fe MOF	Water	Tetracycline	The antibiotic MOF aptamer complex increases the electron transfer resistance and decreases the current flow	0.1–10^5 nM	48.1 ng L^{-1}	105
Electrochemical	AuNP/polyethyleneimine functionalized Fe-MOF	Milk	Tobramycin	The f-probe immobilized on the surface of the MOF competes with the tobramycin to produce current	100 pM to 500 nM	26.2 ng L^{-1}	106
Impedance	Co/Ni MOF	Milk	Enrofloxacin	The antibiotic MOF aptamer complex increases the electron transfer resistance and decreases the current flow	0.001–1 pg mL−1	0.354 μg L^{-1}	107
Immunosensor	Cerium MOF with gold modification	Pork meat	1-Aminohydratoin	Competitive binding of the analyte and antigen to the antibody embedded in the MOF	0.001–1000 μg L^{-1}	1.35×10^{-7} μg L^{-1}	108
Impedance	CoNi MOF derivative	Milk, honey	Furazolidone, chloramphenicol	The aptamer–analyte complex reduces the electron transfer at the electrode surface	—	1.91 μg L^{-1}, 11.31 μg L^{-1}	109
Impedance	Cu–Tb MOF	Milk	Penicillin	The aptamer–analyte complex reduces the electron transfer at the electrode surface resulting in the electrochemical response	—	0.84 pg L^{-1}	110
Electrochemical	Composite of PtPd@Ni–Co hollow nano-boxes (PtPd@Ni–Co HNBs) and poly (diallyldimethylammonium chloride)-functionalized graphene (PDDA-Gr)	Honey	Chloramphenicol	In the presence of CMP, EXO I release a huge amount of trigger DNA (Tr DNA), and this Tr DNA initiates cycle II, which results in the binding of the exposed capture DNA to the signal probes to increase the current flow	10 fM to 10 nM	0.32 pg L^{-1}	111
Impedance	CoNi metallo-covalent organic framework	Milk, chicken egg	Tobramycin	The aptamer analyte complex increases the resistance on the surface of the electrode resulting in reduced electron transfer	—	0.07 fg L^{-1}	112
Impedance	Fe/ZIF-8	Fresh milk	Chloramphenicol and metronidazole	Electrochemical *via* linear sweep voltammetry	0.1–100 μM L^{-1} and 0.5–30 μM L^{-1} respectively	10.6 μg L^{-1} and 28 μg L^{-16}, respectively	78

Table 4 (*Contd.*)

Sensor type	MOF	Sample	Analyte	Mechanism	Linear range	Lod	Reference
Impedance	Ag_2SiF_6-MOF	Aqueous solution	Penicillin	The MOF aptamer antibiotic complex increases the electron transfer resistance of the electrode and decreases the current flow. With the adsorption of penicillin on the surface of the aptamer, MOF NPs, there is a drop in the redox peak of the electrode. The thickening of the electrode with these non-conducting analytes (penicillin) inhibits the electron transfer in the electrode, and hence it detects the varying concentration of penicillin in the solution	0.001 to 0.5 ng mL^{-1}	0.849 pg mL^{-1}	79
Impedance	Ce/Cu-MOF	Milk	Tobramycin	The negatively charged aptamer-analyte specific immunocomplex blocks the electron and mass transfer to the electrode by acting as a blocking layer	0.01 pg mL^{-1} to 10 ng mg L^{-1}	2.0 fg mL^{-1}	77
Impedance	Ce-MOF	Milk	Oxytetracycline	The G quadruplex complex formed between the analyte and aptamer hinders the redox probe access to the electrode	0.1–0.5 ng mL^{-1}	17.4 fg mL^{-1}	82
Electrochemical	Fe_3O_4@mC900	Milk	Oxytetracycline	OTC molecules would interact with aptamers causing less redox probe access to the AE surface and decreasing the electrochemical activity	0.005 to 1.0 ng mL^{-1}	0.027 pg mL^{-1}	83

[a] Abbreviations: DOX – doxycycline, TCT – tetracycline, OCT – oxytetracycline, CTC – chlortetracycline, NFZ – nitrofurazone, NFT – nitrofurantoin, MND – metronidazole, RND – ronidazole, OND – ornidazole, and DND – nitroimidazole.

4.1.1. Luminescence based on ligands. Luminescent organic linkers play a significant role in the design of MOF-based optical sensors and the corresponding detection of a specific analyte. The π electron-rich ligands are the reason for the electron transfer and the subsequent fluorescence. Examples are compounds with tetraphenyl ethylene-, pyrene-, and biphenyl- in their structure. The n → π and π → π* electron transitions also occur within these molecules and hence the luminescence. When combined with metals with an unoccupied d-orbital, the MOF has outstanding performance. These linkers also affect emission along with the electron transition.

Li *et al.* confirmed the huge potential of utilizing multi-pyridinium ligands to synthesize functional MOFs with new and better photophysical properties, for switching and sensing applications of nitrofurans antibiotics. The metallic part is cadmium with a 2D fold, while the carboxylate is the electron donor and pyridinium is the electron acceptor which is the cause of the photochromic nature of the used MOF (due to photo-induced electron transfer). The LOD for nitrofurazone and nitrofurantoin was found to be 39.6 and 62 μg L^{-1} respectively in this work. The broad UV absorption spectra of these materials can be identified as the reason for the fluorescence quenching. There is good overlapping of the light absorption spectra of these nitrofurans with the emission spectra of the MOF thereby inducing an energy transfer from the MOF to antibiotics as well as the extensive overlapping of the absorption spectra of nitrofurans with the excitation spectra of the MOF causing a competitive absorption. Both these overlaps cause fluorescence quenching in 50 s.[63]

A novel cadmium-based MOF with high pH and water media stability has been synthesized by the solvothermal method and one of the first reported methods to detect multiple analytes such as nitrofuran antibiotics, DNC pesticides, ferric ions, and ascorbic acid by turning off fluorescence due to PET and FRET (Fig. 5(A–C)). There is electron transfer from the conduction band of the MOF to the LUMO of nitrofurans (PET) and an extensive overlap of the absorption spectra of nitrofurans with the emission spectra of the MOF (FRET). The detection limit was found to be 50 μg L^{-1} for DND, 80 μg L^{-1} for MND, 100 μg L^{-1} for RND, 81 μg L^{-1} for OND, 137 μg L^{-1} for NFZ, and 262 μg L^{-1} for NFT.[65]

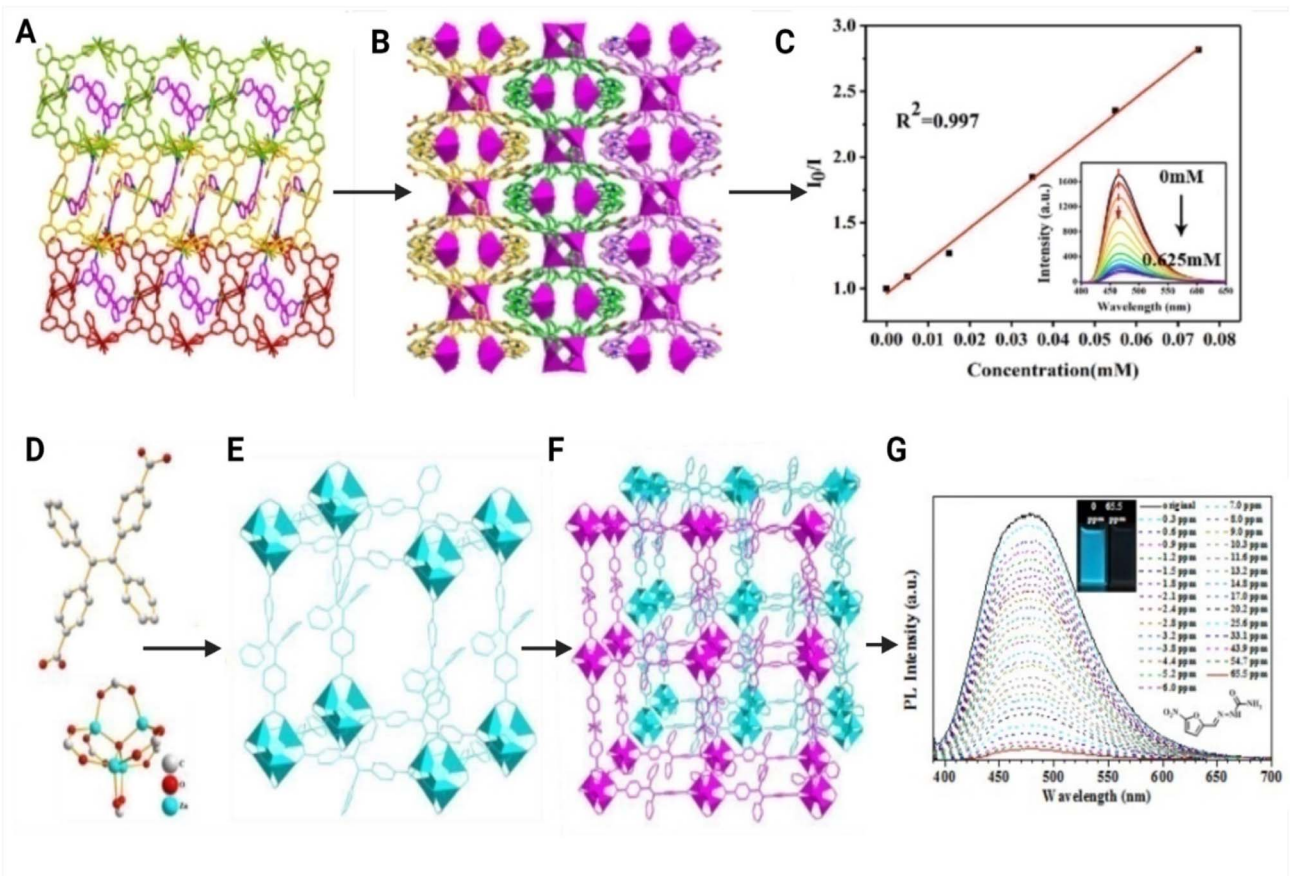

Fig. 5 (A) 2D layer and (B) 3D supramolecular structure of a cadmium-based MOF $[Cd_2(HDDB)(bimpy)(NMP)(H_2O)]\cdot 3H_2O$ where (H_5DDB = 3,5-di(20,40-dicarboxylphenyl)benzoic acid and bimpy = 3,5-bis(1-imidazolyl)pyridine) sensor for the detection of nitrofurans, and (C) fluorescence emission linear spectra of the analyte with the cadmium MOF. Modified and reproduced with permission from the Royal Society of Chemistry.[64] $[Zn_4O(BCTPE)_3]$ MOF where (D) is the structure of the $BCTPE^{2-}$ ligand, (E) is the structure of the $Zn_4O(CO_2)_6$ node, and (F) is the 2-fold crystal structure of the entire MOF. (G) Fluorescence titration of nitrofurazone antibiotic with the MOF. Modified and reproduced with permission from the Royal Society of Chemistry.[69]

A dual MOF with a 3D architecture using aluminium and zinc exhibited brilliant performance and specificity for tetracycline sensing with the inner filter effect and photo-induced electron transfer as the main sensing mechanisms with a wide range of response, ultra-low LOD, and superior selectivity against common interfering compounds such as other antibiotics, amino acids, sugars, some metal ions, and compounds with $-NH_2$ functional groups. All major 4 tetracyclines can be detected using this sensor with LODs of 0.24 μg L^{-1} for doxycycline, 0.25 μg L^{-1} for tetracycline, 0.28 μg L^{-1} for oxytetracycline and 0.44 μg L^{-1} for chlortetracycline. The hydrogen bonding between the OH/COOH of tetracycline with the NH_2 group in this MOF as well as the electron transfer from the MOF to tetracyclines (*via* PET) resulted in effective fluorescence quenching.[64]

A fluorescence turn-on sensor was developed by utilizing the strong coordination between the phosphate backbone of an aptamer and zirconium ions in a bimetallic coordination bonding MOF of UiO-66 and copper. It is a selective and sensitive sensor with a low LOD of 29 ng L^{-1} for the detection of chloramphenicol in fish. In the absence of CMP, the fluorescence of ROX fluorophore is quenched by the MOF as it comes in close contact with the surface when the aptamer is adsorbed on the surface of the MOF through PET. But in the presence of CMP, this close contact is avoided due to the formation of a CMP–aptamer complex with a special spatial structure resulting in fluorescence of ROX detected. The quantity of CMP is proportional to the intensity of fluorescence of ROX.[68] A luminescent MOF of zinc and dicarboxyl-substituted tetraphenylethene (TPE) was reported by Liu *et al.*, for the detection of nitrogen-containing antibiotics such as nitrofurazone and metronidazole with a LOD of 0.1 and 0.6 μg mL^{-1} respectively. The luminescence quenching was attributed to photoinduced electron transfer. The excited-state electron from the highest LUMO of H_2BCTPE gets transferred to those of the analyte because of photoexcitation (Fig. 5(D–G)).[69]

4.1.2. Luminescence based on metals (lanthanides). MOF's luminescence emission can also be caused by metal clusters, such as transition and lanthanide metals. The luminescence of transition metal-based MOFs is due to the organic linker's shift and alteration in the emission peak. This luminescence properties of MOFs depend on the ligand-to-metal electron transfer or metal-to-ligand electron transfer. The energy level of lanthanide metal and organic linkers is approximately the same which results in the 'antenna effect' *via* resonance energy transfer. Thus, they give a characteristic peak of lanthanide ions only. Spin–orbit coupling, electronic repulsion, and the ligand field effect can be used to explain the luminescence of these MOFs.

Chongliang *et al.* reported the development of lanthanide-based MOF (terbium & salicylic acid) test strips which were highly sensitive and the response to the analyte was not hindered by any other components present and the strips were cheap, can be reused at least 6 times, were portable and rapid with a testing time of only 1 minute and were easy to use. The detection was based on the antenna effect *i.e.* the absorption spectra of tetracycline and oxytetracycline (360 nm) overlap with the excitation wavelength of the terbium MOF (361 nm) which resulted in competitive absorption and thereby fluorescence quenching. The MOF was based on the inner filter effect and the LOD was found to be 0.93 μg L^{-1} and 1.37 μg L^{-1} for tetracycline and oxytetracycline respectively.[70]

A bimetallic lanthanide (europium and terbium) MOF was transformed into a luminescent sensor to detect antibiotics for practical uses such as its detection in water. The luminescent study showed that the membranes made from these materials could work as a self-calibrating luminescent probe for various antibiotics in a specific concentration range and it could be used as an inexpensive and convenient prototype sensor to distinctively determine different antibiotics, which enhances its potential practical applications. The limit of detection was found to be 2 μg mL^{-1} and the fluorescence quenching is caused by the overlapping of excitation spectra of the MOF and the absorption spectra of ornidazole as well as the collision between the free ornidazole and MOF resulting in energy transfer.[71]

Jia *et al.* used a real-time MOF sensor with a dye that induces UiO66 encapsulated in SiO_2 and Eu^{3+} for the detection of tetracycline in honey and milk. The LOD was found to be 8.61 μg L^{-1} and the linear range was 0.1–6 μM. The MOF has a blue emission when excited from the dye incorporated. In the presence of tetracycline, a complex is formed between the Eu metal and TC which gave a red emission (617 nm) *via* the 'antenna effect' (Fig. 6(A–C)). This nanoprobe discussed had a LOD of 48.1 μg L^{-1} during onsite detection.[72]

4.2. Colourimetric sensors

Colourimetric sensors are commonly preferred since the presence or absence of an analyte can be identified by the naked eye. The colourimetric sensor works on the principle of a visible colour change. With MOF sensors for antibiotic detection, colourimetry is one area that has not been developed much. Since most MOFs are luminescent, the quenching of this luminescence is utilized as a mechanism of detection vastly. Very few attempts have been made for the development of colourimetric sensors as a result. The few which are developed are based on the enzyme-like catalytic activity of some MOFs such as peroxidase mimetic activity. A chromatic material for *e.g.* 3,3′,5,5′-tetramethylbenzidine (TMB) upon oxidation gives colour to the solution in the presence of chloramphenicol antibiotic residue and Li *et al.* developed such colorimetric detection (Fig. 7(A and B)).[73] The interaction of the aptamer with the analyte caused the reaction of hydrogen peroxide and TMB thereby causing a colour change. The sensor was based on an Fe-MIL-53 MOF and had good intrinsic peroxidase mimetic catalytic activity. AuNPs and the aptamer form a conjugate that is negatively charged and form a layer on the positively charged Fe-MOF. In the absence of antibiotics, there is a change in the colour of the solution from colourless to blue due to the oxidation of TMB in the presence of H_2O_2. In the presence of antibiotics, there is a decrease in catalytic activity due to the unavailability of electron transfer from the Fe MOF to H_2O_2 to form a peroxide radical. The colorimetric sensor based on MOF–aptamer–TMB–

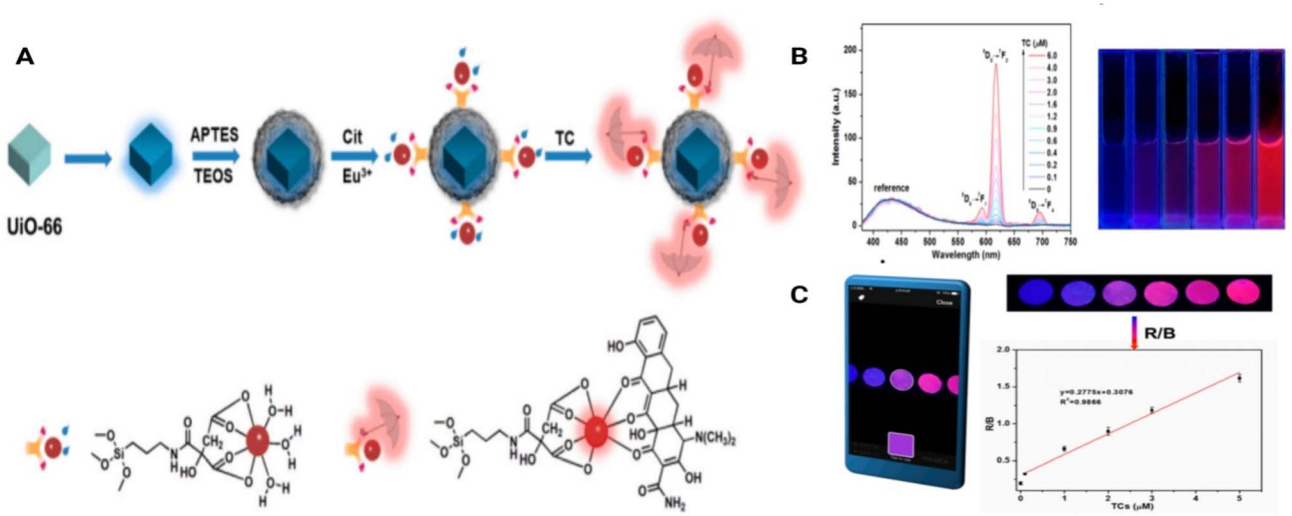

Fig. 6 (A) Fabrication of the Dye@UiO-66-@SiO_2–NH_2-Cit-Eu lanthanide MOF and its sensing of tetracycline, (B) fluorescence spectra and the fluorescence images of the MOF with concentrations of tetracycline antibiotic and (C) the red and blue chromaticity analysis of the fluorescence emission of the MOF with tetracycline calculated using a smartphone. Modified and reproduced with permission from mdpi.[72]

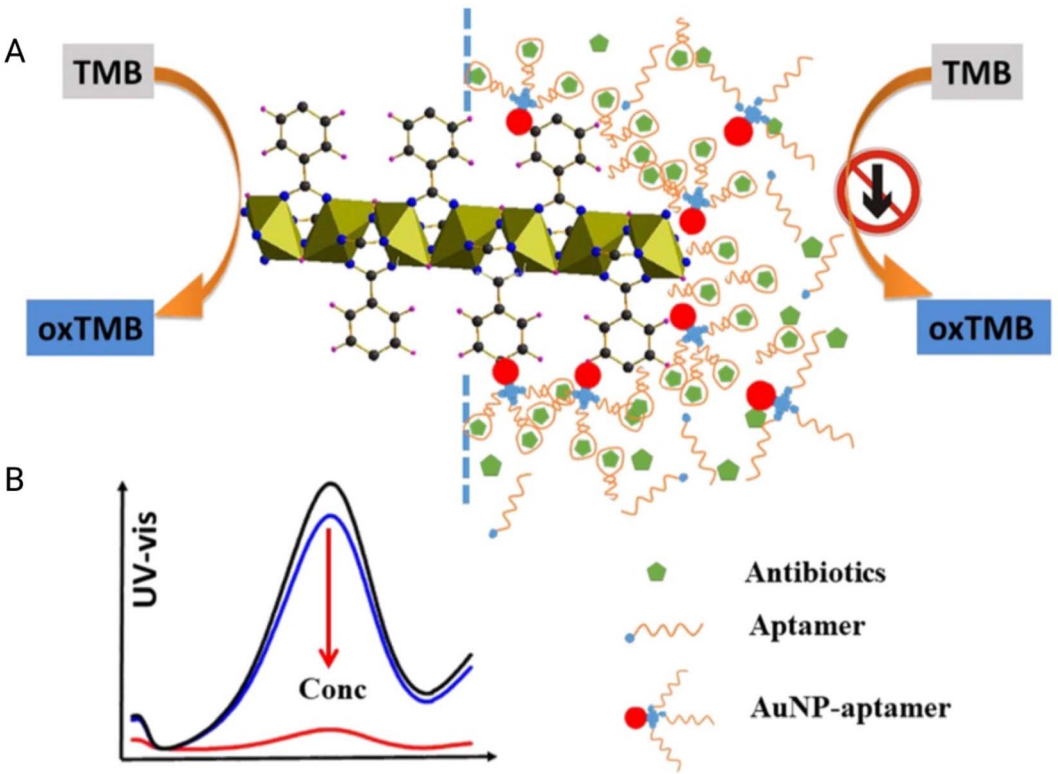

Fig. 7 Colorimetric MOF sensor for chloramphenicol: (A) the schematic design depicting the binding and detection of chloramphenicol based on the antibiotic-aptamer/AuNP-aptamer interaction and enzyme mimetic activity of iron-based MOFs. (B) UV-vis absorbance spectra of the MOF in the presence of various concentrations of CMP. Adapted and reproduced with permission from Elsevier.[73]

H_2O_2 is a highly selective and sensitive and universally applicable sensing platform for antibiotic residue detection in monitoring water quality, but the higher LOD (8.1 ng mL^{-1}) is a drawback in its efficiency in detecting lower concentrations of antibiotics.[73]

The work by Wang *et al.* reported a MOF aptamer colourimetric sensor that was sensitive and selective with excellent accuracy for streptomycin with a streptomycin-specific aptamer which can be replicated for other antibiotics by changing the aptamer sequence for onsite detection of antibiotics in milk.

The sensor contains a zeolitic metal azolate framework-7 (MAF-7) embedded with an antibiotic-specific aptamer and horseradish peroxidase (HRP) enzyme. The enzyme catalytic activity is increased 4 fold in the HRP-MOF composite. This composite oxidizes TMB in the presence of H_2O_2. But in the presence of streptomycin, the aptamer antibiotic complex forms a layer over the HRP-MOF composite, which results in a decrease in catalytic activity. The decrease in intensity is proportional to the concentration of the antibiotic residue. The LOD of this sensor was found to be 0.51 pg L^{-1}, which is less than that of most conventional methods of detection.[74]

5. MOF based electrochemical sensors

Electrochemical sensors are widely used analytical methods due to their high sensitivity, rapid response, *etc.* The operating principle of an electrochemical sensor is the change in current flow due to a chemical reaction on the surface of the electrode.[75] An electrochemical sensor consists of a reference electrode that maintains a constant potential, a counter electrode that closes the circuit between the working electrode and a signal source, and a working electrode at which the reaction takes place.[76] Most electrodes are made using multiple metals and conducting linkers immobilized on glassy carbon electrodes.[77–80] The electrodes are modified by dipping them in MOF suspension for some time and then are dried.[77–80] Based on the literature survey, MOF-based electrochemical sensors for antibiotic residue detection in food are scarce and hence have a lot of room for development.

One of the major issues is the comparatively poor water stability of pristine MOFs since the metal–ligand coordination bonds can be readily cleaved by water molecules and hence often is a limiting factor for electrochemical sensing. From the electroanalytical point of view, MOF functionality is understood through its chemical stability in the targeted electrolytes and the stability of the MOF structures after the completed electroanalytical process. Apart from the MOF thin film deposited on the working electrode surface, metal-coordinated organic linker nodes, supporting electrolytes with varying ionic concentrations, and the buffer solutions used are some of the required parameters in electrochemical sensing operations.

The electrochemical sensing performances of redox-active MOFs can be exhibited by promising redox-active moieties and molecular sites that rely on redox hopping to transport electrons during the electroanalytical processes. Redox hopping is generally combined with both electron transport and the diffusion of active ionic species within the frameworks. However, in certain applications, the characteristic of MOFs with larger pore sizes is not always desirable, because it may decrease the density of active sites, and the active site's electron transport rate and will thus start to limit the overall electrochemical process. But, to achieve a better electroanalytical performance, improving the charge transport within the MOF materials that possess sufficiently large pore sizes for the diffusion of counter ions plays an important role in attaining the targeted analyte detection by this method.

Conducting-type sensors are rarely synthesized using MOFs, and the reason is the presence of bulk organic linkers that are essentially insulators. But recently some attempts have been made to use electrochemical impedance for the detection of antibiotic residues.[78] An aptamer-based electrochemical MOF sensor for enrofloxacin detection was discussed by Song *et al.* where the sensor is based on a semiconducting bimetallic Co/Ni MOF with 2,3,6,7,10,11-hexaiminotriphenylene as the ligand. The LOD of this sensor was found to be as low as 0.2 fg mL^{-1}. The sensing was determined using impedance electrochemistry where sinusoidal alternating current is passed through the solution to measure the total resistance.[81] He *et al.* developed an aptamer-based electrochemical sensor having an Ag MOF for the ultrasensitive detection of penicillin with a LOD of 0.849 pg mL^{-1} in raw milk. The MOF aptamer antibiotic complex increases the electron transfer resistance of the electrode and decreases the current flow. With the adsorption of penicillin on the surface of aptamer-MOF NPs, there is a drop in the redox peak of the electrode. The thickening of the electrode with these non-conducting analytes (penicillin) inhibits the electron transfer in the electrode, and hence it detects the varying concentration of penicillin in the solution.[79]

The analysis of chloramphenicol and metronidazole by using an electrochemical sensor *via* linear sweep voltammetry using an iron, nitrogen co-doped nanoporous carbon–metal–organic framework (type Fe/ZIF-8) on a glassy carbon electrode was also recently discussed by Baikeli *et al.*, in real samples. The complex is simple with a large surface area, mesopores, and particle size. There are three reasons for the electrochemical activity of the Fe/NC framework. They have a large electroactive surface area, fine conductivity of the Fe/NC framework, and the catalysis of Fe atoms to chloramphenicol and metronidazole. The reported LOD was 10.6 μg L^{-1} and 28.6 μg L^{-1} for chloramphenicol and metronidazole respectively.[78] Wang *et al.* also developed a bimetallic cerium/copper aptamer-based MOF for the ultra-sensitive detection of tobramycin in milk which had a LOD of 2.0 fg mL^{-1}. The MOF-modified aptamer electrode is used as the working electrode, a platinum wire as the counter electrode, Ag/AgCl as the reference electrode, and a 1 : 1 mixture of $K_3[Fe(CN)_6]/K_4[Fe(CN)_6]$ as a redox probe. The aptamer–analyte complex reduces the diffusion of $Fe(CN)_6^{3-/4-}$ to the electrode surface resulting in a reduced current flow.[77] A hybrid nanocomposite aptasensor of a porous organic framework and cerium-MOF for the detection of oxytetracycline in milk was described by Zhou *et al.* as seen in Fig. 8(A and B). The LOD for this sensor was found to be 17.4 fg mL^{-1} and the linear range to be 0.1–0.5 ng mL^{-1}. Melamine and cyanuric acid monomers are the precursors used in the synthesis of this organic framework. There is a strong interaction between the aptamer strands and the nanocomposite, which helps in the immobilization of aptamers and subsequent analyte absorption. An A-G DNA quadruplex complex is formed between the oxytetracycline and the aptasensor due to the amide bond, which decreases the redox signal of the electrode because of steric hindrance by the formed complex. The electrochemical changes were measured

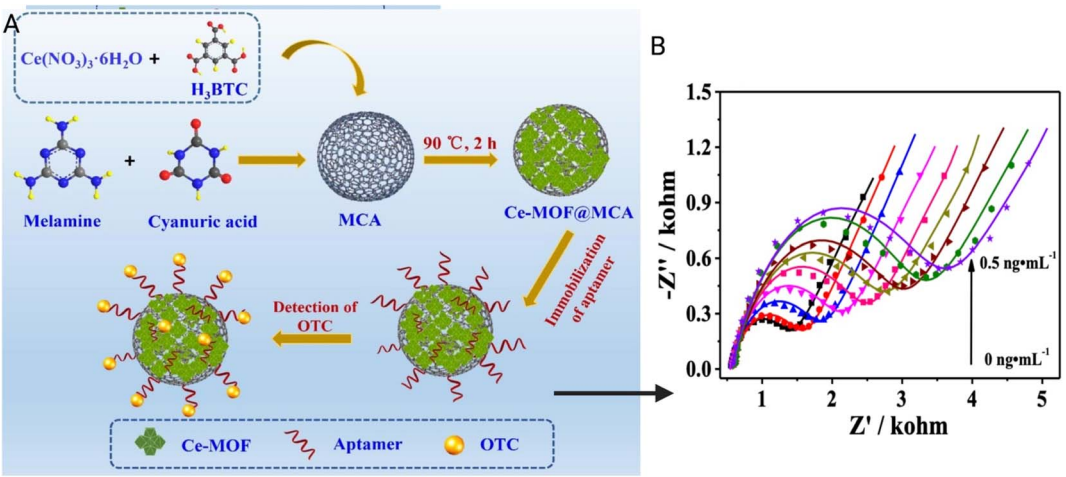

Fig. 8 (A) Schematic diagram of the fabrication procedure of the Ce-MOF@MCA-based aptasensor for detecting oxytetracycline (OTC). (B) Nyquist plots for the detection of different concentrations of OTC using the Ce-MOF@MCA_{500}-based aptasensor. Modified and reproduced with permission from Elsevier.[82]

using electrochemical impedance spectroscopy.[82] Song *et al.* described an oxytetracycline sensor with a LOD of 0.027 pg mL^{-1} and a linear range between 0.005 and 1.0 ng mL^{-1}. The gold electrode is used as a working electrode, Ag/AgCl as a reference electrode, and a platinum slide as a counter electrode. An Fe_3O_4 mesoporous carbon was coated on the working electrode along with an oxytetracycline-specific aptamer. The oxytetracycline forms a G-quadruplex complex with the aptamer, which results in low redox probe access to the working electrode which decreases the electrochemical activity.[83]

6. Recent advancements

6.1. Hydrothermal and solvothermal method of MOF synthesis for antibiotic detection

A hydrothermally synthesized 3D green, fluorescent terbium MOF was reported by Liu *et al.*, for the detection of tetracycline in milk with a LOD of 88.5 μg L^{-1} with a broad linear range of 0–100 and 100–244 μM L^{-1}. This is highly selective and sensitive with a very low LOD and a rapid response time of just 2 min. The mechanism of quenching was described as the inner filter effect and FRET. It was found that there is a broad overlap of the absorption spectra of TC and the excitation spectra of the MOF. The competitive absorption of the excitation wavelength of the MOF by the TC causes the quenching of fluorescence. Another reason for quenching found with the peak analyzer was the possibility of the formation of a H bond between the OH/COOH group of TC with the NH_2 group in the MOF resulting in energy transfer from the ligand to Tb^{3+}.[91] A one-step hydrothermally synthesized luminescent fusiform aluminum MOF for the detection of nitrofuran in milk was also reported by Yue *et al.*, where the LOD was discovered to be 105, 200, and 131 μg L^{-1} for nitrofurazone, nitrofurantoin, and furazolidone respectively. The inner filter effect *i.e.* the spectral overlap of the excitation wavelength and absorption spectra of nitrofuran was depicted as the mechanism of detection. They also extended the work by developing a paper test strip for semi-quantitative detection of nitrofuran onsite by the naked eye where the blue colour of the paper strip decreases with an increase in nitrofuran concentration.[90]

Recent advancements in MOF sensors for antibiotic detection include a solvothermally synthesized 3D europium MOF with wide pH stability (3–12) as discussed by Wang *et al.*, which can rapidly detect metronidazole and dimetridazole with recyclability and a LOD of 13 μg L^{-1} (metronidazole) and 13.4 μg L^{-1} (dimetridazole) in lake water (Fig. 9(C and D)).[86] The mechanism was found to be due to the transfer of electrons from the conduction band of the MOF to the LUMO of analytes (*via* PET) and overlapping of the UV spectra of the analyte and MOF, which results in fluorescence quenching.[86] This MOF can be further modified to analyze antibiotic residues in food, feed, and water.

6.2. Competitive, ratiometric, and overlapping fluorescence quenching mechanism-based MOF sensors for antibiotic detection

Lei *et al.*, developed a 3D porous Tb MOF sensor with a urea-modified tetracarboxylic ligand with a wide pH range (2–14) for the detection of multiple antibiotics with two distinct emission peaks for urea (400 nm) and Tb^{3+} (540 nm) such as nitrofurans, nitroimidazoles, and sulphonamides (Fig. 9(A–C)).[96] Though it detects multiple antibiotic classes, the detection mechanism is different. Nitrofurans such as nitrofurantoin and nitrofurazone have given maximum quenching when detected but sulphonamides with this MOF have given enhanced fluorescence, particularly with sulphamethoxazole. The ratio of luminescence intensity at 544 nm and 400 nm is utilized for calculating the concentration of analytes instead of total fluorescence. In the detection of nitrofurans and nitroimidazoles, the selectivity is based on the intensity difference in the ratio between strong emission at 544 nm and weak emission at 400 nm. The nitro group containing antibiotics

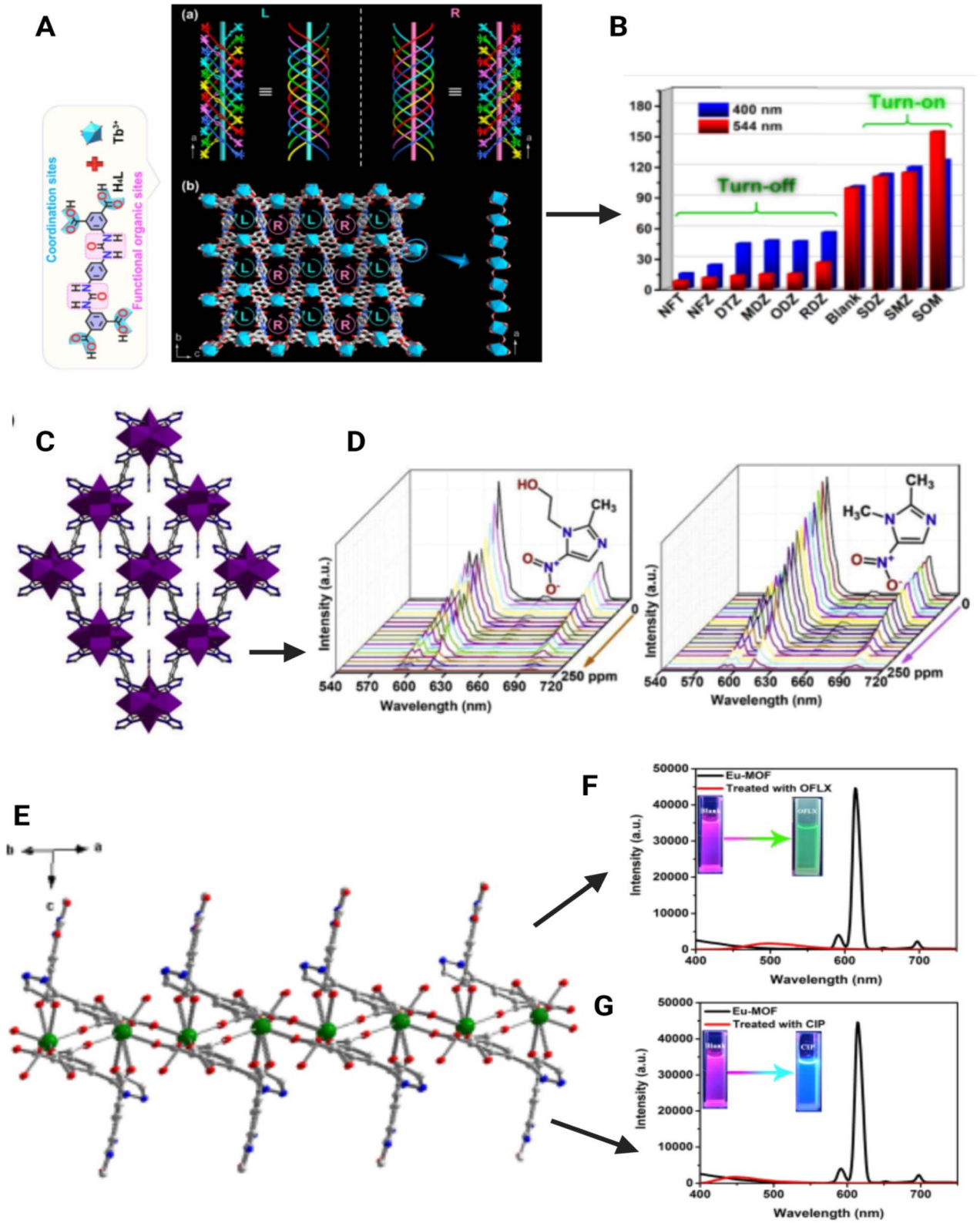

Fig. 9 (A) Double-stranded helical structure of the Tb-MOF along the *a*-axis with right and left views. (B) The related luminescence intensity of Tb-MOF with different antibiotics. Modified and reproduced with permission from the American Chemical Society.[96] (C) $[Eu_2(dtztp)(OH)_2(DMF)(H_2O)_{2.5}]\cdot 2H_2O$ MOF 3D framework and (D) fluorescence bands of the above-mentioned MOF upon addition of metronidazole and dimetridazole antibiotics respectively. Modified and reproduced with permission from Elsevier.[86] (E) 2D network structure of Eu-MOF, and (F) and (G) the fluorescence spectra comparison and colour change when Eu-MOF is added with ciprofloxacin and ofloxacin antibiotics respectively. Modified and reproduced with permission from the American Chemical Society.[92]

acts as an electron acceptor and the ligands as an electron donor causing fluorescence quenching, but sulfamethoxazole has a higher LUMO than the ligand and therefore acts as an electron donor and causes fluorescence enhancement. The other sulpha drugs have similar LUMO ligands and hence no electron transfer. The other cause of quenching is the competitive absorption of the excitation wavelength by both analytes and ligands in the case of nitrofurans and nitroimidazoles. The LOD of nitrofurantoin is 98 μg L^{-1} and that of dimetridazole is 196 μg L^{-1}.[96]

A new europium-based MOF was described by Xiao *et al.*, for the selective detection of ciprofloxacin and ofloxacin which had a LOD of 0.693 ng L^{-1} and 0.802 ng L^{-1} respectively (Fig. 9(E–G)).[92] The fluorescence quenching is caused by PET and the dynamic quenching mechanism. At low concentrations, there is no formation of a complex but at higher concentrations, there is

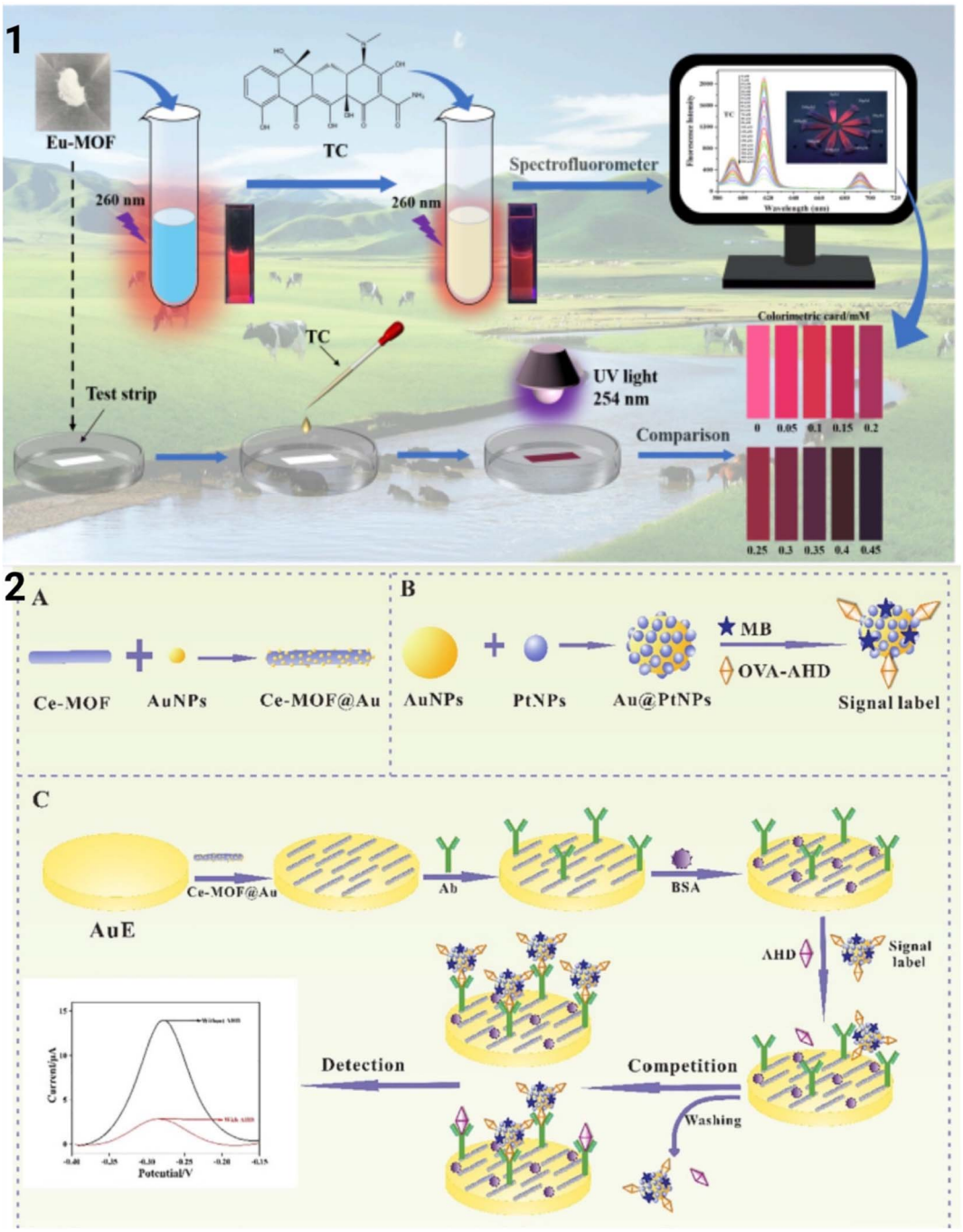

Fig. 10 (1) Eu MOF-based portable test strip for rapid and visual detection of tetracycline based on a simple spectrofluorometer. Reproduced with permission from Elsevier.[87] (2) Detection of nitrofurantoin metabolite 1-aminohydantoin using Ce-MOF@Au by the electrochemical immunosensing technique. Reproduced with permission from Elsevier.[108]

a complex formation. There is also electron transfer from the LUMO of the analyte and the LUMO of the ligand in the Eu MOF (*via* PET). This sensor is a very powerful tool for the detection of the above antibiotics as it helps in rapid detection, and easy identification with the naked eye, and has a low LOD. The red emission of MOF changes to blue in the presence of ciprofloxacin and changes to green in the presence of ofloxacin.[86] A ratiometric sensor comprising zeolitic imidazolate framework-8 incorporated with gold clusters and green-emitting carbon dots with dual emissions for the detection of cephalexin in milk is developed. The gold cluster has an emission wavelength of 630 nm and green-emitting carbon dots have an emission of 520 nm when excited at 400 nm. The cephalexin selectively quenches the emission of the gold cluster while the fluorescence of carbon dots remains the same. It can be noted that the ratio of emission (F_{520}/F_{630}) is linearly proportional to the concentration of the analyte. This linear relationship is seen in the range of 0.1–6 ng L^{-1} and the detection limit was found to be 0.04 ng L^{-1}.[88] The europium MOF was developed for the detection of tetracycline in milk and beef with a LOD of 19.1 μg L^{-1}. This MOF has red fluorescence at 617 nm when excited at 260 nm. In the presence of tetracycline, the fluorescence is quenched and can be distinguished with the naked eye. The inner filter effect (overlapping of excitation spectra of the MOF and absorption spectra of the analyte) and PET (transfer of an electron from the MOF to the analyte) were considered to be the reason for quenching. Furthermore, importantly a test strip using this MOF was made with deposition on the MOF on a paper surface. This can be used for the onsite detection of tetracycline (Fig. 10(1)).[87]

6.3. Designer aptamer-based MOF sensors for antibiotic detection

A multiplexed antibiotic residue sensor was developed by Chen *et al.*, where metal ions based signal aptamer, capture and assisted Y-DNA probes were electrochemically utilized with MOF NPs to distinguish chloramphenicol and oxytetracycline residues in food sample.[84] Cd^{2+} and Pb^{2+} metal ions with their respective signal DNA were collectively conjugated to the Zr-MOF NPs and then the respective capture aptamers were made to form complementary strands along with the assisted DNA probes attached on the gold NP surface. Together, the assisted DNA probe, the capture aptamer probe and the signal DNA probe with the MOF formed the Y-shaped DNA complex which dissembled and underwent circular strand replacement polymerization reaction in the presence of the analytes. The developed electrochemical sensor did not have any cross reactivity, had enhanced signal output because of the replenished use of the ions, and was specific for chloramphenicol and oxytetracycline residues in milk samples (LOD 0.033 and 0.048 pM respectively).

Zhang *et al.* developed an aptasensor for the detection of tobramycin using electrochemically deposited gold nanoparticles coordinated with polyethyleneimine functionalized Fe-MOF. The LOD was found to be 56 pM and the linear range to be 100 pM to 500 nM. An f-probe (complementary DNA strand to tobramycin aptamer) was immobilized on the surface of the MOF along with the aptamer. In the absence of TOB, the f-probe and aptamer form a complete DNA structure so that very little current flows. But, in the presence of TOB, the f probe remains unhybridized and a very high current flow is observed. This current flow is proportional to the concentration of TOB.[106] A heterometallic MOF of copper and terbium with DMF as a ligand was employed for the detection of penicillin in milk. This electrochemical aptasensor has a LOD of 0.84 pg mL^{-1}, which can be considered very low and can be considered highly sensitive. The aptamer–analyte complex reduces the electron transfer on the surface of the electrode by increasing the resistance. This reduced current flow is proportional to the concentration of penicillin. The recovery range of penicillin in milk by the MOF was between 100.3 and 113.4%. This indicates that this sensor can accurately determine penicillin in raw milk.[110] An electrochemical aptasensor with a composite of PtPd@Ni–Co hollow nano-boxes (PtPd@Ni–Co HNBs) and poly (diallyldimethylammonium chloride)-functionalized graphene (PDDA-Gr) was developed for ultrasensitive detection of chloramphenicol (CMP) and was tested in honey. In the presence of CMP, EXO I releases a huge amount of trigger DNA (Tr DNA), and this Tr DNA initiates cycle II, which results in the binding of the exposed capture DNA to the signal probes to increase the current flow. This aptasensor has a wide linear range (10 fM to 10 nM) and a detection limit of 0.32 pg L^{-1}.[111]

A simple, rapid, selective, sensitive, and low-cost aptasensor for the detection of tetracycline using an Fe MOF(NH_2-MIL-101(Fe)/CNF@AuNPs) was synthesized using the combination of 4 different methods such as hydrothermal, electrospinning, pyrolysis, and electrodeposition resulting in increased sensitivity to the analyte. In the presence of TC, the aptamer–analyte complex on the surface of the electrode reduces the electron transfer on the surface of the electrode due to impedance resulting in reduced current. The LOD of this sensor was found to be 48.1 ng L^{-1} and under optimum conditions, there is a linear relationship between impedance and concentration ($0.1–10^5$ nM).[105]

6.4. Electrochemiluminescent, analyte derivative, and molecularly imprinted polymer-based MOF sensors for antibiotic detection

A deeper understanding of nitrofuran antibiotics in biological systems provided the idea that they have a very short life span in the living system, and they are converted to their amino derivates. One such derivative of nitrofurantoin is 1-aminohydratoin (AHD), which was used as a target analyte for detection in pork by Wang *et al.*, using a competitive-type electrochemical immunosensor recently. A core–shell dual MOF was used for this with Ce-MOF functionalized with gold particles (Ce-MOF@Au) to improve its electrical conductivity and methylene blue loaded gold platinum (MB-Au@Pt) embedded with an antigen (OVA AHD) as a label. The working electrode is modified with Ce-MOF@Au and the detection is based on competitive immunosensing. The AHD when introduced competes with the antigen for the AHD antibody causing

a reduction in signal response. This sensor has a very low LOD of 1.35×10^{-7} μg L^{-1} with a linear range of 0.001–1000 μg L^{-1} (Fig. 10(2)).[108]

An electrochemiluminescent aptasensor for the detection of kanamycin was discussed by Wen *et al.*, with gold-incorporated HKUST(Au@HKUST) with a cysteine perylene derivative (PTC-Cys)/peroxydisulfate ($S_2O_8^{2-}$) with an ultra-low LOD of 20.34 pg L^{-1}. The MOF part of the sensor acts as a catalyst for the electrochemical reduction of $S_2O_8^{2-}$ to a sulfate radical anion. In the presence of the analyte, the complex of analyte–aptamer enhances the electrochemiluminescence as it pulls the aptamer from the surface. The cysteine perylene used here is a luminophore. This is a highly selective sensitive stable sensor and can be used for monitoring food safety and was demonstrated using milk with a recovery rate of 96.5–101.72%.[85]

The first-ever attempt at simultaneous detection of furazolidone and chloramphenicol using a modified glassy carbon electrode using bimetallic Co/Ni MOF-derived hollow $NiCo_2O_4$ in milk and honey was discussed by Xia Niu and the team. The LOD of FZD was found to be 1.91 μg L^{-1} and 11.31 μg L^{-1} for CMP. Mechanism studies show that there is a reduction of both analytes on the surface of the electrode *via* a four-electron four proton process causing an increase in current flow. The experiments on milk and honey give appreciable results and hence it can be used for monitoring the quality of these products.[109] Amiripour *et al.* presented a new idea of incorporating a nanostructured molecular imprinted polymer (MIP) coated luminescent zirconium MOF with a CMP template for the detection of chloramphenicol in milk and honey. The sensor has many recognition sites and hence selective absorption of CMP on the surface of the MOF with the help of a MIP. Acceptable recoveries were obtained from the real samples with a LOD of 0.013 μg L^{-1} and a linear range of 0.16–161.56 μg L^{-1}. In the presence of CMP, there is non-homogenous adsorption of CMP on the MOF surface, and this interaction enhances the fluorescence of the MOF, *i.e.* in the presence of CMP, there is a turn on of the fluorescence of the MOF.[88]

7. Future prospects and discussion

Antibiotic residues have already made an impact within agro-food systems due to their prevalence in a variety of foods and beverages meant for human consumption. Ben *et al.* in their review have detailed the recent summary of various antibiotic residues in food products and food systems which is briefed out next.[8] Antibiotic residues such as quinolones, chloramphenicol, sulfonamides, and macrolides have already been detected in drinking water; in meat products derived from antibiotic drug exposed food animals in various countries, multiple residues such as sulfonamides and tetracyclines have been found in the liver of chicken, beef, and swine at higher concentrations, while fishes and shrimps showed quinolone and sulfonamide antibiotic residues being the most detected; numerous antibiotic residues have been simultaneously found in milk and dairy products with the highest concentration of chloramphenicol and penicillin G being detected in milk from China and Nigeria respectively; highest concentrations of chlortetracycline in egg white and yolk; quinolones and chloramphenicol were also found in vegetables and edible crops with the antibiotic residues generally being distributed in the order of leaf > stem > root in plants.[8] A recent study published in 2023 analyzed various fertilizer samples that were produced from pig and poultry manure, slurry and digestate and recorded a dominant presence of doxycycline (with soil microorganism threatening levels of 175 mg kg^{-1} in pig manure) apart from oxytetracycline, tetracycline, lincomycin, tiamulin and enrofloxacin.[113] Overall, there is an urgent need as well as demand for the routine detection and quantification of these veterinary antibiotic residues in various food matrices from the interest of consumer safety and public health. This makes MOFs as reliable materials for developing sensors that can perform the detection of these residues on a routine basis below the limits set by regulation bodies.

MOF sensors for antibiotic residue detection so far vastly employed luminescence/fluorescence quenching mechanisms since most MOFs are fluorescent or luminescent and this ability is used to detect various antibiotic residues in numerous food samples. Developing MOFs by utilizing aggregation-induced emission luminous (AIEgens) as organic linkers (AIE-MOFs) is another aspect that could in the future be used to develop AIEgens activity-based sensors that show simple and effective ''turn-on'' responses for analytes with the limited label or label-free approach for antibiotic detection.[114,115] As seen, these novel nanomaterials have a very low LOD and excellent selectivity mainly because of their nanoscale porosity which offers internal high sensibility, the molecular sieve effect of the uniformly distributed cavities, and the exposed ligands present contribute towards selective recognition.[115] In this way, MOFs are tunable and specifically designed for selective sensing purposes. But certain limitations persist with these materials considering that MOFs are difficult to synthesize in a controlled fashion and the procurement of various framework components can be expensive. The size, shape, and porosity all are critical factors that enable a MOF material to sense an analyte and it is still difficult to precisely control these parameters during synthesis. This provides the opportunity to explore many more new synthesis routes that would allow the facile reproduction of these MOFs. For example, most of the MOF's synthesis involves conventional solvothermal methods, which involve solvent-based reactions of metal ions with organic linkers and subsequent crystallization in a closed vessel where high temperature and pressure (above the boiling point of a solvent) facilitate self-assembly and crystal growth.[116] Alternative to this is mechano-chemical methods which have gained new traction lately as a green and cost-effective route of MOF synthesis. This method involves high-speed grinding of metal and organic ligands in a ball mill, which results in a shorter reaction time, less energy consumption, high yield of MOF material, and easy scale up as well.[116] The recent advance in this method includes the use of a small quantity of solution, which helps in the movement of metal ions and ligands that subsequently improves the reaction. Most solvents used in the conventional synthesis route are hazardous. Hence this method which particularly is solvent-free or uses a very small quantity of solvent is advantageous.

Moreover, the use of ionic and supercritical liquids in this method is highly efficient in dissolving organic and inorganic materials and helps in the synthesis of new architectures in MOFs. Supercritical fluids help in structure direction and modification as well.[117] Flow synthesis is another method recently developed for the synthesis of MOFs. The most important advantage of this method is the ability to control the size by *in situ* UV absorption spectroscopy. The characterization and size monitoring of MOFs in fluid media is often very difficult to achieve. Li *et al.* introduced an integrated system of a flow synthesis system produced by femtosecond laser micromachining and UV spectroscopy where the size of the crystal ranged from 200–1025 nm.[118] All these synthesis advancements can also be extended toward developing MOFs specifically for antibiotic residue detection.

Due to the insulating properties of most of the organic ligands, the electrochemical properties of MOFs are also poor, and not much study has been conducted in these areas where novel electrochemical transduction systems have been explored. Few latest studies are being conducted to improve the conductivity of MOFs with nanosheet and nanowire architectures. Realistic electrochemical-based sensors can be attained by improving the conductivity and design of redox-active MOF materials by introducing non-native conductive functional materials such as metal nanoparticles, carbon nanostructures, polymers, and biomolecules into MOF porous structures in a synergistic manner to improve the overall performance of the resulting MOF nanocomposite.[119] For example, Chen *et al.* reported for the first time the integration of Pt nanocrystals (known for catalytic oxidation of alcohol and the photothermal effect in surface plasmon resonance) into a porphyrinic MOF (known to be an effective photosensitizer for $^1O_2$ generation) producing a MOF nanocomposite Pt/PCN-224(Zn) that showed such excellent and selectively enhanced catalytic activity towards photooxidation of aldehydes in aromatic alcohol oxidation by 1 atom O_2 at ambient temperature.[120] Here, PCN-224(Zn) exhibited the greatest ability for O_2 activation and $^1O_2$ production because of strong diamagnetism from Zn^{2+} compared to other residing metals in the porphyrin MOF, whereas the electronic state of Pt NPs can be tuned to light-intensity for O_2 activation based on competition between its Schottky junction and plasmonic effect. Similarly, Wang *et al.* had developed a Cu@HUKAST-1 MOF nanocomposite *via in situ* etching and the resulting composite had enhanced photothermal catalytic activity for a one-pot cascade reaction.[121] Such strategic examples can be realized to develop functional MOF based electrochemical electrodes when combined with multivalent ligands and metal nodes to enhance their redox activity, controlled immobilization methods for stable signal amplification and the introduction of many functional groups for water stability.[119] Hence, this offers many more opportunities to explore new methods specifically for antibiotic residue detection.

Another major concern is water stability and pH stability of MOFs. The MOFs with metal and nitrogen-containing ligands are more alkaline stable whereas the metal–oxygen bond is acid-stable.[119] The instability of MOFs in water can be addressed by using hydrophobic functional groups or making the coordinate bonds between the metal node and ligand more functionally robust. Conventional synthesis methods with large particle sizes have always been one of the biggest disadvantages in the development of MOFs with unique properties. A new method of synthesis was described by Guoyu Wei and team which was termed the microplasmic electrochemical strategy.[124] In this method, a modified electrochemical method is employed for the synthesis of a very common MOF, HKUST-1, in a rapid and controlled synthesis manner. A 10 mA current was discharged for 15 min using a microplasma cathode in a precursor solution of cupric nitrate and 1,3,5-benzene tricarboxylic acid dissolved in DMF in a H-type reaction equipment. The mesoporous diameter of the obtained MOF was calculated using the Barrett–Joyner–Halenda method and was found to be 1.8 nm. The concentration, current discharge, *etc.* have a proportional relation to the amount of MOF synthesized.[124] These latest studies such as the microplasma electrochemistry strategy and mechano-chemical methods are promising steps toward synthesizing stable and highly efficient MOFs. Some of them also take leaps towards the green synthesis of MOFs so that less hazardous chemicals are used. It is also worth noting that most sensors have not ventured into testing in real-life samples. The detection in most cases is based on the overlapping of the emission spectra and the absorption spectra of the antibiotic *i.e.*, the photons emitted by the MOF during emission are directly absorbed by the analyte and hence there is fluorescence quenching.[122] But in some rare cases, the excitation wavelength of the MOF and the absorption wavelength of antibiotics overlap with each other, thereby causing competitive absorption. This can lead to decreased excitation and therefore less emission. The scenario with a higher concentration of antibiotics is different. Researchers suggest that at a high concentration of antibiotics, there may be the formation of a complex of antibiotics and the MOF with a chemical bond, but the structure and nature of these complexes are yet to be studied. The mechanism of fluorescence quenching caused by this complex is also unknown.

Most electrochemical sensors utilize the resistance created by the presence of antibiotic–aptamer complexes as the most prominent mechanism. The MOF in the absence of an analyte conducts electricity but has an innate resistance. When antibiotic molecules are present in the sample, the total resistance of the solution increases compared to the pristine MOF reagent due to the redox reaction which may be observed as a reduction in the working electrode current flow. Hence, this new resistance/impedance also decreases the current flow through the solution. This change in current flow is measured and used for the quantification of antibiotic residues. Although MOFs identify target analytes through their interactions *via* hydrogen bonding, π–π interactions, open metal sites, and van der Waals interactions,[119] more studies should be carried out to understand the complexity of its mechanism of sensing and the nature and stability of MOF-antibiotic complexes. Along with this, the complexity of food matrices and difficult clean-up procedures contribute to the reason why these materials were not used to perform real-life sample analysis in many studies.

Very few of the reported MOF sensors have made it into real-life testing, and most of them have focused only on milk samples which can be considered a common food product. More researchers must focus on developing sensors for other food products such as meat, seafood, eggs, offals, vegetables, and edible crops along with many processed products as well.

Ideally, a good sensor, in this case, would be the use of a MOF nanomaterial (or nanocomposite) that could serve as a platform for multiplexed antibiotic residue detection and quantification in a single sample. Research should also focus on developing a MOF nanocomposite-based surface-enhanced Raman spectroscopic (SERS) method for antibiotic residue detection in food since Raman spectroscopy is capable of even label-free, single-target molecule fingerprinting. A recent study has used a magnetic MOF nanocomposite such as Au/Fe_3O_4/MIL-101(Cr) as a SERS substrate for antibiotic residue detection in environmental samples.[125] Such studies can also be extended towards food samples for rapid molecular-level detection. Although several attempts have been successfully made as mentioned in the previous section, further efforts could also be conceptualized with MOF nanomaterial integrated lab-on-chip technology such as integrated molecular spectroscopy, array-type sensors, and optical fiber-based sensors for a feasible simultaneous, individual discrimination of each antibiotic residue and its quantification for real-time, on-site, routine food sample analysis.[60,123]

8. Conclusion

Metal–organic frameworks (MOFs) are a class of porous hybrid nanomaterials formed by networks of inorganic metal ions or metal clusters that can be tuned for unique optical, electrochemical, and optoelectronic properties for the highly selective detection of various classes of antibiotics. MOFs have huge advantages over other materials in many properties for the detection of antibiotics, such as strong sensitivity, selectivity, specific designs, and multiple attachment sites for functional groups, portability, and operability. Their porous structures are also helpful in the controllability of luminescence intensity *via* the analyte–receptor interaction. As a result, many MOF sensors have reported LOD values at very low levels of ng and pg thus allowing for the lowest discrimination of these residues in a sample. To improve the performance of the MOF's sensor properties, the necessary functional groups will be grafted to MOFs through selective binding/interaction sites using different physisorption and chemisorption interactions. They have broad and large potential use in the food supply chain for the trace detection of antibiotic residues that are currently a global threat. The quenching of fluorescence of MOF materials is the main principle utilized so far for the detection of antibiotic residues. The interaction between the antibiotic molecules and MOF needs further exploration for a better understanding and the elucidation of their recognition mechanisms would shed more light on the chemistry of detection. Electrochemical sensors should also receive more attention for further development considering that they would offer excellent selectivity and sensitivity when combined with the inherent superior properties of MOFs. Future research should focus on more real-life sample testing as well as towards routine onsite detection with these sensors. More upcoming research should focus on combining MOFs as sensing materials with portable devices so that scaling up these sensors would show commercial feasibility. Despite all the above-discussed pros, they also have several limitations that restrict their commercial applications, such as poor water stability, dispersibility, and unclear self-assembly which would eventually hamper their rational fabrication. Also, it is worth noting that most of the research involving MOFs for antibiotic residue detection has solely focused only on the methodology and have not ventured into real-time sample analysis. By addressing these issues, the growing catalogue of MOF material-based sensors has huge prospects ahead and can be a very promising material for multiple antibiotic residue detection for various food matrices.

Conflicts of interest

The authors declare no conflict of interest financial or otherwise.

Abbreviations

CMP	Chloramphenicol
CTC	Chlortetracycline
DNA	Deoxyribose nucleic acid
DOX	Doxycycline
ELISA	Enzyme-linked immune sorbent assay
FL	Fluorescence
FRET	Fluorescence energy transfer
FSSAI	Food safety and standard authority of India
GI	Gastrointestinal tract
HOMO	Higher occupied molecular orbital
HPLC	High-performance liquid chromatography
HRP	Horse radish peroxide
IFE	Inner filter effect
LC-MS	Liquid chromatography-mass spectroscopy
LCTEM	Liquid cell tandem electron microscopy
LOD	Limit of detection
LU	Luminescence
LUMO	Lower unoccupied molecular orbital
MND	Metronidazole
MOF	Metal–organic framework
MRL	Maximum residue limit
NFT	Nitrofurantoin
NFZ	Nitrofurazone
NPs	Nanoparticles
OND	Ornidazole
OTC	Oxytetracycline
PET	Photo-electron transfer
PSM	Post-synthetic modification
RET	Resonance energy transfer
RND	Ronidazole
ROX	6-Carboxy-*x*-rhodamine
TC	Tetracyclines

TCT	Tetracycline
TEM	Tandem electron microscopy
TMB	3,3′,5,5′-Tetramethylbenidine

Acknowledgements

This review article was supported by the National Institute of Food Technology Entrepreneurship and Management (NIFTEM), set up by the Ministry of Food Processing Industries (MoFPI), Government of India at HSIIDC Industrial Estate, Kundli in Sonipat district of Haryana which comes under Delhi NCR.

References

1 M. D. Mund, U. H. Khan, U. Tahir, B. E. Mustafa and A. Fayyaz, Antimicrobial drug residues in poultry products and implications on public health: A review, *Int. J. Food Prop.*, 2017, **20**(7), 1433–1446, DOI: 10.1080/10942912.2016.1212874.

2 T. T. H. Van, Z. Yidana, P. M. Smoker and P. J. Coloe, Antibiotic Use in Food Animals in theWorld with Focus on Africa: Pluses and Minuses, *J. Global Antimicrob. Resist.*, 2020, **20**, 170–177, DOI: 10.1016/j.jgar.2019.07.031.

3 M. Bacanlı and N. Başaran, Importance of antibiotic residues in animal food, *Food Chem. Toxicol.*, 2019, **125**, 462–466, DOI: 10.1016/j.fct.2019.01.033.

4 T. P. V. Boeckel, E. Emma, D. Chen, M. Gilbert, T. P. Robinson, B. T. Grenfell, S. A. Levin and S. Bonhoeffer, Reducing antimicrobial use in food animals, *Insights*, 2017, **357**(6358), 2–5, DOI: 10.1126/science.aao14.

5 M. Gbylik-sikorska, A. Posyniak, T. Sniegocki and J. Zmudzki, Chemosphere Liquid chromatography-tandem mass spectrometry multiclass method for the determination of antibiotics residues in water samples from water supply systems in food-producing animal farms, *Chemosphere*, 2015, **119**, 8–15, DOI: 10.1016/j.chemosphere.2014.04.105.

6 Y. Feng, W. Zhang, Y. Liu, J. Xue and Z. Li, A Simple, Sensitive, and Reliable Method for the Simultaneous Determination of Multiple Antibiotics in Vegetables through SPE-HPLC- MS/MS, *Molecules*, 2018, **23**, 1953, DOI: 10.3390/molecules23081953.

7 X. Yu, H. Liu, C. Pu, J. Chen, Y. Sun and L. Hu, Determination of multiple antibiotics in leafy vegetables using QuEChERS–UHPLC–MS/MS, *J. Sep. Sci.*, 2018, **41**(3), 713–722, DOI: 10.1002/jssc.201700798.

8 Y. Ben, C. Fu, M. Hu, L. Liu, M. H. Wong and C. Zheng, Human Health Risk Assessment of Antibiotic Resistance Associated with Antibiotic Residues in the Environment: A Review, *Environ. Res.*, 2018, **169**, 483–493, DOI: 10.1016/j.envres.2018.11.040.

9 B. Du, F. Wen, Y. Zhang, N. Zheng, S. Li, F. Li and J. Wang, Presence of tetracyclines, quinolones, lincomycin, and streptomycin in milk, *Food Control*, 2019, **100**, 171–175, DOI: 10.1016/j.foodcont.2019.01.00.

10 J. Chen, G. G. Ying and W. J. Deng, Antibiotic Residues in Food: Extraction, Analysis, and Human Health Concerns, *J. Agric. Food Chem.*, 2019, **67**(27), 7569–7586, DOI: 10.1021/acs.jafc.9b01334.

11 B. K. S. Khanal, M. B. Sadiq, M. Singh and A. K. Anal, Screening of antibiotic residues in fresh milk of Kathmandu valley, Nepal, *J. Environ. Sci. Health, Part B*, 2018, **53**(1), 57–86, DOI: 10.1080/03601234.2017.1375832.

12 I. O. Olatoye, O. F. Daniel and S. A. Ishola, Screening of antibiotics and chemical analysis of penicillin residue in fresh milk and traditional dairy products in Oyo state, Nigeria, *J. Environ. Sci. Health, Part B*, 2016, **9**, 948–954, DOI: 10.14202/vetworld.2016.948-954.

13 S. Chowdhury, M. M. Hassan, M. Alam, S. Sattar and S. Bari, Antibiotic residues in milk and eggs of commercial and local farms atChittagong, Bangladesh, *Vet. World*, 2015, **8**, 467–471, DOI: 10.14202/vetworld.2015.467-471.

14 M. A. Hebbal, C. Latha, K. Vrinda Menon and J. Deepa, Occurrence of oxytetracycline residues in milk samples from Palakkad, Kerala, India, *Vet. World*, 2020, **13**(6), 1056–1064, DOI: 10.14202/vetworld.2020.1056-1064.

15 C. Willis, Antibiotics in the food chain: their impact on the consumer, *Rev. Med. Microbiol.*, 2000, **11**, 153–160, DOI: 10.1097/00013542-200011030-00005.

16 B. Ghorbani, M. Ghorbani, M. Abedi and M. Tayebi, Effect of Antibiotics Overuse in Animal Food and its Link with Public Health Risk, *Int. J. Sci. Res. Sci. Technol.*, 2016, **2**(1), 46–50, DOI: 10.1007/s00604-016-1896-2.

17 Z. E. Menkem, B. L. Ngangom, S. S. A. Tamunjoh and F. F. Boyom, Antibiotic residues in food animals: Public health concern, *Acta Ecol. Sin.*, 2019, **39**(5), 411–415, DOI: 10.1016/j.chnaes.2018.10.004.

18 N. Tarannum, S. Khatoon and B. B. Dzantiev, Perspective and application of molecular imprinting approach for antibiotic detection in food and environmental samples : A critical review, *Food Control*, 2020, **118**, 107381, DOI: 10.1016/j.foodcont.2020.107381.

19 M. K. Rayappa, A. P. Viswanathan, G. Rutta and P. M. Krishna, Nanomaterials Enabled and Bio/Chemical Analytical Sensors for Acrylamide Detection in Thermally Processed Foods: Advances and Outlook, *J. Agric. Food Chem.*, 2021, **69**, 4578–4603, DOI: 10.1021/acs.jafc.0c07956.

20 X. Fang, B. Zong and S. Mao, Metal-Organic Framework-Based Sensors for Environmental Contaminant Sensing, *Nano-Micro Lett.*, 2018, **10**(4), 1–19, DOI: 10.1007/s40820-018-0218-0.

21 L. Liu, Y. Zhou, S. Liu and M. Xu, The Applications of Metal À Organic Frameworks in Electrochemical Sensors, *ChemElectroChem*, 2018, **5**, 6–19, DOI: 10.1002/celc.201700931.

22 A. Amini, S. Kazemi and V. Safarifard, Metal-organic framework-based nanocomposites for sensing applications - A Review, *Polyhedron*, 2019, 114260, DOI: 10.1016/j.poly.2019.114260.

23 L. E. Kreno, K. Leong, O. K. Farha, M. Allendorf, D. R. P. Van and J. T. Hupp, Metal-organic framework materials as chemical sensors, *Chem. Rev.*, 2012, **112**(2), 1105–1125, DOI: **10.1021/cr200324t**.

24 S. Pal, S. S. Yu and C. W. Kung, Group 4Metal-Based Metal-organic frameworks for chemical sensors, *Chemosensors*, 2021, **9**, 306, DOI: **10.3390/chemosensors9110306**.

25 M. Chauhan, S. K. Bhardwaj, G. Bhanjana, R. Kumar, N. Dilbaghi, S. Kumar and G. R. Chaudhary, Chapter 3 - Conducting Polymers and Metal-Organic Frameworks as Advanced Materials for the Development of Nanosensors, *Advances in nanosensors for biological and environmental analysis*, Elsevier Inc., 2019, pp. 43–62, DOI: **10.1016/B978-0-12-817456-2.00003-6**.

26 L. Du, W. Chen, P. Zhu, Y. Tian, Y. Chen and C. Wu, Applications of Functional Metal-Organic Frameworks in Biosensors, *Biotechnol. J.*, 2021, **16**(2), 1900424, DOI: **10.1002/biot.201900424**.

27 J. Lei, R. Qian, P. Ling, L. Cui and H. Ju, Design and sensing applications of metal-organic framework composites, *TrAC, Trends Anal. Chem.*, 2014, **58**, 71–78, DOI: **10.1016/j.trac.2014.02.012**.

28 F. Sun, Z. Yin, Q. Q. Wang, D. Sun, M. H. Zeng and M. Kurmoo, Tandem post-synthetic modification of a metal-organic framework by thermal elimination and subsequent bromination: Effects on absorption properties and photoluminescence, *Angew. Chem., Int. Ed.*, 2013, **52**(17), 4538–4543, DOI: **10.1002/anie.201300821**.

29 W. Xia, J. Zhu, W. Guo, L. An, D. Xia and R. Zou, Well-defined carbon polyhedrons prepared from nano metal-organic frameworks for oxygen reduction, *J. Mater. Chem. A*, 2014, **2**(30), 11606–11613, DOI: **10.1039/c4ta01656d**.

30 H. Bunzen, M. Grzywa, M. Hambach, S. Spirkl and D. Volkmer, From Micro to Nano: A Toolbox for Tuning Crystal Size and Morphology of Benzotriazolate-Based Metal-Organic Frameworks, *Cryst. Growth Des.*, 2016, **16**(6), 3190–3197, DOI: **10.1021/acs.cgd.6b00038**.

31 X. Dou, K. Sun, H. Chen, Y. Jiang, L. Wu, J. Mei, Z. Ding and J. Xie, Nanoscale metal-organic frameworks as fluorescence sensors for food safety, *Antibiotics*, 2021, **10**, 4, DOI: **10.3390/antibiotics10040358**.

32 Z. Q. Li, A. Wang, C. Y. Guo, Y. F. Tai and L. G. Qiu, One-pot synthesis of metal-organic framework@SiO2 core-shell nanoparticles with enhanced visible-light photoactivity, *Dalton Trans.*, 2013, **42**(38), 13948–13954, DOI: **10.1039/c3dt50845e**.

33 R. C. Arbulu, Y. B. Jiang, E. J. Peterson and Y. Qin, Metal-Organic Framework (MOF) Nanorods, Nanotubes, and Nanowires, *Angew. Chem., Int. Ed.*, 2018, **57**(20), 5813–5817, DOI: **10.1002/anie.201802694**.

34 R. Li, W. Wang, E. S. M. El-Sayed, K. Su, P. He and D. Yuan, Ratiometric fluorescence detection of tetracycline antibiotic based on a polynuclear lanthanide metal-organic framework, *Sens. Actuators, B*, 2021, **330**, 129314, DOI: **10.1016/j.snb.2020.129314**.

35 N. Xu, Q. Zhang and G. Zhang, A carbazole-functionalized metal-organic framework for efficient detection of antibiotics, pesticides, and nitroaromatic compounds, *Dalton Trans.*, 2019, **48**(8), 2683–2691, DOI: **10.1039/c8dt04558e**.

36 J. Xiong, L. Yang, L. X. Gao, P. P. Zhu, Q. Chen and K. J. Tan, A highly fluorescent lanthanide metal-organic framework as a dual-mode visual sensor for berberine hydrochloride and tetracycline, *Anal. Bioanal. Chem.*, 2019, **411**(23), 5963–5973, DOI: **10.1007/s00216-019-02004-9**.

37 J. D. Sosa, T. F. Bennett, K. J. Nelms, B. M. Liu, R. C. Tovar and Y. Liu, Metal–Organic Framework Hybrid Materials and Their Applications, *Crystals*, 2018, **8**(8), 325, DOI: **10.3390/cryst8080325**.

38 J. Cravillon, R. Nayuk, S. Springer, A. Feldhoff, K. Huber and M. Wiebcke, Controlling zeolitic imidazolate framework nano- and microcrystal formation: Insight into crystal growth by time-resolved *in situ* static light scattering, *Chem. Mater.*, 2011, **23**(8), 2130–2141, DOI: **10.1021/cm103571y**.

39 N. T. K. Thanh, N. Maclean and S. Mahiddine, Mechanisms of nucleation and growth of nanoparticles in solution, *Chem. Rev.*, 2014, **114**(15), 7610–7630, DOI: **10.1021/cr400544s**.

40 J. P. Patterson, P. Abellan, M. S. Denny, C. Park, N. D. Browning, S. M. Cohen, J. E. Evans and N. C. Gianneschi, Observing the Self-assembly of Metal-Organic Frameworks by In-Situ Liquid Cell TEM, *Microsc. Microanal.*, 2015, **21**(S3), 2445–2446, DOI: **10.1017/s1431927615013008**.

41 S. Surblé, F. Millange, C. Serre, G. Férey and R. I. Walton, An EXAFS study of the formation of a nanoporous metal-organic framework: Evidence for the retention of secondary building units during synthesis, *Chem. Commun.*, 2006, **14**, 1518–1520, DOI: **10.1039/b600709k**.

42 Y. Zhu, J. Ciston, B. Zheng, X. Miao, C. Czarnik, Y. Pan, R. Sougrat, Z. Lai, C. E. Hsiung and K. Yao, Unraveling surface and interfacial structures of a metal-organic framework by transmission electron microscopy, *Nat. Mater.*, 2017, **16**(5), 532–536, DOI: **10.1038/NMAT4852**.

43 S. Hermes, T. Witte, T. Hikov, D. Zacher, S. Bahnmüller, G. Langstein, K. Huber and R. Fischer, Trapping Metal-Organic Framework Nanocrystals: An in-Situ Time-Resolved Light Scattering Study on the Crystal Growth of MOF-5 in Solution, *J. Am. Chem. Soc.*, 2007, **129**(17), 5324–5325, DOI: **10.1021/ja068835i.s001**.

44 S. Wang, C. M. McGuirk, A. d'Aquino, J. A. Mason and C. A. Mirkin, Metal-Organic Framework Nanoparticles, *Adv. Mater.*, 2018, **30**(37), 1–14, DOI: **10.1002/adma.201800202**.

45 F. Alexis, E. Pridgen, L. K. Molnar and O. C. Farokhzad, Reviews: Factors Affecting the Clearance and Biodistribution of Polymeric Nanoparticles, *Mol. Pharm.*, 2008, **5**(4), 505–515, DOI: **10.1021/mp800051m**.

46 S. Li and L. Huang, Reviews: Pharmacokinetics and Biodistribution of Nanoparticles, *Mol. Pharm.*, 2008, **5**(4), 496–504, DOI: **10.1021/mp800049w**.

47 N. I. Gonzalez-Pech and V. H. Grassian, Surface Chemical Functionalities of Environmental Nanomaterials,

Reference Module in Chemistry, Molecular Sciences and Chemical Engineering, 2017, DOI: 10.1016/b978-0-12-409547-2.13188-9.

48 A. G. Dong, X. C. Ye, J. Chen, Y. J. Kang, T. Gordon, J. M. Kikkawa and C. B. Murray, A generalized ligand-exchange strategy enabling sequential surface functionalization of colloidal nanocrystals, *J. Am. Chem. Soc.*, 2011, **133**, 998–1006.

49 Q. Q. Dai, D. M. Li, H. Y. Chen, S. H. Kan, H. D. Li, S. Y. Gao, Y. Y. Hou, B. B. Liu and G. T. Zou, Colloidal CdSe nanocrystals synthesized in noncoordinating solvents with the addition of a secondary ligand: exceptional growth kinetics, *J. Phys. Chem. B*, 2006, **110**, 16508–16513.

50 A. Prakash, H. Zhu, C. J. Jones, D. N. Benoit, A. Z. Ellsworth, E. L. Bryant and V. L. Colvin, Bilayers as phase transfer agents for nanocrystals prepared in nonpolar solvents, *ACS Nano*, 2009, **3**, 2139–2146.

51 W. Yang, Y. Wang, J. Li and X. R. Yang, Polymer wrapping technique: an effective route to prepare Pt nanoflower/carbon nanotube hybrids and application in oxygen reduction, *Energy Environ. Sci.*, 2010, **3**, 144–149.

52 W. W. Yu, E. Chang, J. C. Falkner, J. Y. Zhang, A. M. Al-Somali, C. M. Sayes, J. Johns, R. Drezek and V. L. Colvin, Forming biocompatible and non aggregated nanocrystals in water using amphiphilic polymers, *J. Am. Chem. Soc.*, 2007, **129**, 2871–2879.

53 J. Nam, N. Won, J. Bang, H. Jin, J. Park, S. Jung, Y. Park and S. Kim, Surface engineering of inorganic nanoparticles for imaging and therapy, *Adv. Drug Delivery Rev.*, 2013, **65**, 622–648.

54 S. Ravindran and C. S. Ozkan, Self-assembly of ZnO nanoparticles to electrostatic coordination sites of functionalized carbon nanotubes, *Nanotechnology*, 2005, **16**, 1130–1136.

55 A. M. Dennis, D. C. Sotto, B. C. Mei, I. L. Medintz, H. Mattoussi and G. Bao, Surface ligand effects on metal-affinity coordination to quantum dots: implications for nanoprobe self-assembly, *Bioconjugate Chem.*, 2010, **21**, 1160–1170.

56 R. Mejia-Ariza and J. Huskens, Formation of hybrid gold nanoparticle network aggregates by specific host-guest interactions in a turbulent flow reactor, *J. Mater. Chem. B*, 2014, **2**, 210–216.

57 Y. Shi, H. Zhang, Z. Yue, Z. Zhang, K. S. Teng, M. J. Li, C. Q. Yi and M. S. Yang, Coupling gold nanoparticles to silica nanoparticles through disulfide bonds for glutathione detection, *Nanotechnology*, 2013, **24**(37), 375501.

58 N. Manousi, D. A. Giannakoudakis, E. Rosenberg and G. A. Zachariadis, Extraction of Metal Ions with Metal–Organic Frameworks, *Molecules*, 2019, **24**(24), 4605, DOI: 10.3390/molecules24244605.

59 S. Ramanayaka, M. Vithanage, A. Sarmah, T. An, K. H. Kim and Y. S. Ok, Performance of metal–organic frameworks for the adsorptive removal of potentially toxic elements in a water system: a critical review, *RSC Adv.*, 2019, **9**(59), 34359–34376, DOI: 10.1039/C9RA06879A.

60 M. Z. H. Khan, Recent Biosensors for Detection of Antibiotics in Animal Derived Food, *Crit. Rev. Anal. Chem.*, 2020, 1–11, DOI: 10.1080/10408347.2020.1828027.

61 H. Y. Li, S. N. Zhao, S. Q. Zang and J. Li, Functional metal-organic frameworks as effective sensors of gases and volatile compounds, *Chem. Soc. Rev.*, 2020, **49**(17), 6364–6401, DOI: 10.1039/c9cs00778d.

62 X. D. Zhu, K. Zhang, Y. Wang, W. W. Long, R. J. Sa, T. F. Liu and J. Lü, Fluorescent Metal-Organic Framework (MOF) as a Highly Sensitive and Quickly Responsive Chemical Sensor for the Detection of Antibiotics in Simulated Wastewater, *Inorg. Chem.*, 2018, **57**(3), 1060–1065, DOI: 10.1021/acs.inorgchem.7b02471.

63 P. Li, M. Y. Guo, L. L. Gao, X. M. Yin, S. L. Yang, R. Bu and E. Q. Gao, Photoresponsivity and antibiotic sensing properties of an entangled tris(pyridinium)-based metal-organic framework, *Dalton Trans.*, 2020, **49**(22), 7488–7495, DOI: 10.1039/D0DT00397B.

64 C. Li, W. Yang, X. Zhang, Y. Han, W. Tang, T. Yue and Z. Li, A 3D hierarchical dual-metal-organic framework heterostructure up-regulating the pre-concentration effect for ultrasensitive fluorescence detection of tetracycline antibiotics, *J. Mater. Chem. C*, 2020, **8**(6), 2054–2064, DOI: 10.1039/C9TC05941E.

65 D. Feng, J. Tang, J. Yang, X. Ma, C. Fan and X. Wang, A multi-responsive luminescent probe of antibiotics, pesticides, Fe3+, and ascorbic acid with a Cadmium(II) metal-organic framework, *J. Mol. Struct.*, 2020, **1221**, 128841, DOI: 10.1016/j.molstruc.2020.128841.

66 C. Li, X. Zhang, S. Wen, R. Xiang, Y. Han, W. Tang, T. Yue and Z. Li, Interface engineering of zeolite imidazolate framework−8 on two-dimensional Al−metal−organic framework nanoplates enhancing performance for simultaneous capture and sensing tetracyclines, *J. Hazard. Mater.*, 2020, **395**, 122615, DOI: 10.1016/j.jhazmat.2020.12261.

67 J. Wang, Q. Zha, G. Qin and Y. Ni, A novel Zn(II)-based metal-organic framework as a highly selective and sensitive sensor for fluorescent detections of aromatic nitrophenols and antibiotic metronidazole, *Talanta*, 2020, **211**, 120742, DOI: 10.1016/j.talanta.2020.120742.

68 Z. Lu, Y. Jiang, P. Wang, W. Xiong, B. Qi, Y. Zhang, D. Xiang and K. Zhai, Bimetallic organic framework-based aptamer sensors: a new platform for fluorescence detection of chloramphenicol, *Anal. Bioanal. Chem.*, 2020, **412**(22), 5273–5281, DOI: 10.1007/s00216-020-02737-y.

69 X. G. Liu, C. L. Tao, H. Q. Yu, B. Chen, Z. Liu, G. P. Zhu, Z. Zhao, L. Shen and B. Z. Tang, A new luminescent metal-organic framework based on dicarboxyl-substituted tetraphenylethene for efficient detection of nitro-containing explosives and antibiotics in aqueous media, *J. Mater. Chem. C*, 2018, **6**(12), 2983–2988, DOI: 10.1039/c7tc05535h.

70 L. Chongliang, C. Zeng, Z. Chen, Y. Jiang, H. Yao, Y. Yang and W. T. Wong, Luminescent lanthanide metal-organic framework test strip for immediate detection of

tetracycline antibiotics in water, *J. Hazard. Mater.*, 2020, **384**, 121498, DOI: 10.1016/j.jhazmat.2019.121498.

71 J. Dong, S. L. Hou and B. Zhao, Bimetallic Lanthanide-Organic Framework Membranes as a Self-Calibrating Luminescent Sensor for Rapidly Detecting Antibiotics in Water, *ACS Appl. Mater. Interfaces*, 2020, **12**(34), 38124–38131, DOI: 10.1021/acsami.0c09940.

72 L. Jia, S. Guo, J. Xu, X. Chen, T. Zhu and T. Zhao, A ratiometric fluorescent nano-probe for rapid and specific detection of tetracycline residues based on a dye-doped functionalized nanoscaled metal-organic framework, *Nanomaterials*, 2019, **9**(7), 976, DOI: 10.3390/nano9070976.

73 J. Li, C. Yu, Y. N. Wu, Y. Zhu, J. Xu, Y. Wang, H. Wang, M. Guo and F. Li, Novel sensing platform based on gold nanoparticle-aptamer and Fe-metal-organic framework for multiple antibiotic detections and signal amplification, *Environ. Int.*, 2019, **125**, 135–141, DOI: 10.1016/j.envint.2019.01.033.

74 L. Wang, G. Liu, Y. Ren, Y. Feng, X. Zhao, Y. Zhu, M. Chen, F. Zhu, Q. Liu and X. Chen, Integrating Target-Triggered Aptamer-Capped HRP@Metal-Organic Frameworks with a Colorimeter Readout for On-Site Sensitive Detection of Antibiotics, *Anal. Chem.*, 2020, **92**(20), 14259–14266, DOI: 10.1021/acs.analchem.0c03723.

75 M. Majdinasab, K. Mitsubayashi and J. L. Marty, Optical and Electrochemical Sensors and Biosensors for the Detection of Quinolones, *Trends Biotechnol.*, 2019, **37**(8), 898–915, DOI: 10.1016/j.tibtech.2019.01.004.

76 N. S. Alsaiari, K. Katubi, F. M. Alzahrani, S. M. Siddeeg and M. A. Tahoon, The Application of Nanomaterials for the Electrochemical Detection of Antibiotics: A Review, *Micromachines*, 2021, **12**(3), 308, DOI: 10.3390/mi12030308.

77 S. Wang, Z. Li, F. Duan, B. Hu, L. He, M. Wang, N. Zhou, Q. Jia and Z. Zhang, Bimetallic cerium/copper organic framework-derived cerium and copper oxides embedded by mesoporous carbon: Label-free aptasensor for ultrasensitive tobramycin detection, *Anal. Chim. Acta*, 2019, **1047**, 150–162, DOI: 10.1016/j.aca.2018.09.064.

78 Y. Baikeli, X. Mamat, F. He, X. Xin, Y. Li, H. A. Aisa and G. Hu, Electrochemical determination of chloramphenicol and metronidazole by using a glassy carbon electrode modified with iron, nitrogen co-doped nanoporous carbon derived from a metal-organic framework (type Fe/ZIF-8), *Ecotoxicol. Environ. Saf.*, 2020, **204**, 111066, DOI: 10.1016/j.ecoenv.2020.111066.

79 H. He, S. Q. Wang, Z. Y. Han, X. H. Tian, W. W. Zhang, C. P. Li and M. Du, Construction of electrochemical aptasensors with Ag(I) metal−organic frameworks toward high-efficient detection of ultra-trace penicillin, *Appl. Surf. Sci.*, 2020, **531**(I), 147342, DOI: 10.1016/j.apsusc.2020.147342.

80 Y. Tian, Y. Chen, M. Chen, Z. L. Song, B. Xiong and X. B. Zhang, Peroxidase-like Au@Pt nanozymeas an integrated nanosensor for Ag+ detection by LSPR spectroscopy, *Talanta*, 2021, **221**, 121627, DOI: 10.1016/j.talanta.2020.121627.

81 Y. Song, M. Xu, X. Liu, Z. Li, C. Wang, Q. Jia, Z. Zhang and M. Du, A label-freeenrofloxacin electrochemical aptasensor constructed by a semiconducting CoNi-based metal-organic framework (MOF), *Electrochim. Acta*, 2021, **368**, 137609, DOI: 10.1016/j.electacta.2020.137609.

82 N. Zhou, Y. Ma, B. Hu, L. He, S. Wang, Z. Zhang and S. Lu, Construction of Ce-MOF@COF hybrid nanostructure: Label-free aptasensor for the ultrasensitive detection of oxytetracycline residues in aqueous solution environments, *Biosens. Bioelectron.*, 2019, **127**, 92–100, DOI: 10.1016/j.bios.2018.12.024.

83 Y. Song, F. Duan, S. Zhang, J. Y. Tian, Z. Zhang, Z. W. Wang, C. Liu, X. W. M. Sen and M. Du, Iron oxide@mesoporous carbon architectures derived from a Fe(II)-based metal-organic framework for highly sensitive oxytetracycline determination, *J. Mater. Chem. A*, 2017, **5**(36), 19378–19389, DOI: 10.1039/C7TA03959J.

84 M. Chen, N. Gan, T. Li, Y. Wang, Q. Xu and Y. Chen, An electrochemical aptasensor for multiplex antibiotics detection using Y-shaped DNA-based metal ions encoded probes with NMOF substrate and CSRP target-triggered amplification strategy, *Anal. Chim. Acta*, 2017, **968**, 30–39, DOI: 10.1016/j.aca.2017.03.024.

85 J. Wen, L. Zhou, D. Jiang, X. Shan and W. Wang, Analytica Chimica Acta Ultrasensitive ECL aptasensing of kanamycin based on synergistic Au @ HKUST-1, *Anal. Chim. Acta*, 2021, **1180**, 338780, DOI: 10.1016/j.aca.2021.338780.

86 G. D. Wang, Y. Z. Li, W. J. Shi, B. Zhang, L. Hou and Y. Y. Wang, A robust cluster-based Eu-MOF as a multi-functional fluorescence sensor for detection of antibiotics and pesticides in water, *Sens. Actuators, B*, 2021, **331**, 129377, DOI: 10.1016/j.snb.2020.129377.

87 Z. Gan, X. Hu, X. Xu, W. Zhang, X. Zou, J. Shi, K. Zheng and M. Arslan, A portable test strip based on a fluorescent europium-based metal-organic framework for rapid and visual detection of tetracycline in food samples, *Food Chem.*, 2021, **354**, 129501, DOI: 10.1016/j.foodchem.2021.129501.

88 R. Jalili, M. H. Irani-Nezhad, A. Khataee and S. W. Joo, A ratiometric fluorescent probe based on carbon dots and gold nanocluster encapsulated metal-organic framework for detection of cephalexin residues in milk, *Spectrochim. Acta, Part A*, 2021, **262**, 120089, DOI: 10.1016/j.saa.2021.120089.

89 F. Amiripour, S. Ghasemi and S. N. Azizi, Design of turn-on luminescent sensor based on nanostructured molecularly imprinted polymer-coated zirconium metal-organic framework for selective detection of chloramphenicol residues in milk and honey, *Food Chem.*, 2021, **347**, 129034, DOI: 10.1016/j.foodchem.2021.129034.

90 X. Yue, Z. Zhou, M. Li, M. Jie, B. Xu and Y. Bai, Inner-filter effect induced fluorescent sensor based on fusiform Al-MOF nanosheets for sensitive and visual detection of nitrofuran in milk, *Food Chem.*, 2022, **367**, 130763, DOI: 10.1016/j.foodchem.2021.130763.

91 X. Liu, Q. Ma, X. Feng, R. Li and X. Zhang, A recycled Tb-MOF fluorescent sensing material for highly sensitive and

selective detection of tetracycline in milk, *Microchem. J.*, 2021, **170**, 106714, DOI: 10.1016/j.microc.2021.106714.

92 J. Xiao, M. Liu, F. Tian and Z. Liu, 2021. Stable Europium-based Metal-Organic Frameworks for Naked-eye Ultrasensitive Detecting Fluoroquinolones Antibiotics, *Inorg. Chem.*, 2021, **60**(7), 5282–5289, DOI: 10.1021/acs.inorgchem.1c00263.

93 G. Qin, L. Li, W. Bai, Z. Liu, F. Yuan and Y. Ni, Highly sensitive and visualized sensing of nitrofurazone on 2D Tb3+@Zn-AIP ultrathin nanosheets, *Dyes Pigm.*, 2021, **190**, 109309, DOI: 10.1016/j.dyepig.2021.109309.

94 Z. D. Zhou, C. Y. Wang, G. S. Zhu, Y. Y. Jiao, B. Y. Yu and C. C. Wang, Water-Stable Europium(III) and Terbium(III)–Metal-Organic Frameworks as Fluorescent Sensors to Detect Inorganic Ions, Antibiotics and Pesticides in Aqueous Solutions, *SSRN*, 2022, **1251**, 132009, DOI: 10.2139/ssrn.3912003.

95 R. Xie, P. Yang, J. Liu, X. Zou, Y. Tan, X. Wang, J. Tao and P. Zhao, Lanthanide-functionalized metal-organic frameworks based ratiometric fluorescent sensor array for identification and determination of antibiotics, *Talanta*, 2021, **231**, 122366, DOI: 10.1016/j.talanta.2021.122366.

96 M. Lei, F. Ge, X. Gao, Z. Shi and H. Zheng, A Water-Stable Tb-MOF As a Rapid, Accurate, and Highly Sensitive Ratiometric Luminescent Sensor for the Discriminative Sensing of Antibiotics and D2O in H2O, *Inorg. Chem.*, 2021, **60**(14), 10513–10521, DOI: 10.1021/acs.inorgchem.1c01145.

97 R. Wu, C. Bi, D. Zhang, C. Fan, L. Wang, B. Zhu, W. Liu, N. Li, X. Zhang and Y. Fan, Highly selective, sensitive, and stable three-dimensional luminescent metal-organic framework for detecting and removing of the antibiotic in an aqueous solution, *Microchem. J.*, 2020, **159**, 105349, DOI: 10.1016/j.microc.2020.105349.

98 F. Guo, C. Su, Y. Fan, W. Shi and X. Zhang, Construction of a dual-response luminescent metal-organic framework with excellent stability for detecting Fe3+ and antibiotics with high selectivity and sensitivity, *J. Solid State Chem.*, 2020, **284**, 121183, DOI: 10.1016/j.jssc.2020.121183.

99 L. Yu, H. Chen, J. Yue, X. Chen, M. Sun, J. Hou, K. A. Alamry, H. M. Marwani, X. Wang and S. Wang, Europium metal-organic framework for selective and sensitive detection of doxycycline based on fluorescence enhancement, *Talanta*, 2020, **207**, 120297, DOI: 10.1016/j.talanta.2019.120297.

100 Q. Liu, D. Ning, W. J. Li, X. M. Du, Q. Wang, Y. Li and W. J. Ruan, Metal-organic framework-based fluorescent sensing of tetracycline-type antibiotics applicable to environmental and food analysis, *Analyst*, 2019, **144**(6), 1916–1922, DOI: 10.1039/C8AN01895B.

101 Y. M. Ying, C. L. Tao, M. Yu, Y. Xiong, C. R. Guo, X. G. Liu and Z. Zhao, *In situ* encapsulation of pyridine-substituted tetraphenylethene cations in a metal-organic framework for the detection of antibiotics in the aqueous medium, *J. Mater. Chem. C*, 2019, **7**(27), 8383–8388, DOI: 10.1039/c9tc02229e.

102 L. Yu, H. Chen, J. Yue, X. Chen, M. Sun, H. Tan, A. M. Asiri, K. A. Alamry, X. Wang and S. Wang, Metal-Organic Framework Enhances Aggregation-Induced Fluorescence ofChlortetracycline and the Application for Detection, *Anal. Chem.*, 2019, **91**(9), 5913–5921, DOI: 10.1021/acs.analchem.9b00319.

103 Q. Yang, L. Zhou, Y. X. Wu, K. Zhang, Y. Cao, Y. Zhou, D. Wu, F. Hu and N. Gan, A two-dimensional metal-organic framework nanosheets-based fluorescence resonance energy transfer aptasensor with circular strand-replacement DNA polymerization target-triggered amplification strategy for homogenous detection of antibiotics, *Anal. Chim. Acta*, 2018, **1020**, 1–8, DOI: 10.1016/j.aca.2018.02.058.

104 M. L. Han, G. X. Wen, W. W. Dong, Z. H. Zhou, Y. P. Wu, J. Zhao, D. S. Li, L. F. Ma and X. Bu, A heterometallic sodium-europium-cluster-based metal-organic framework as a versatile and water-stable chemosensor for antibiotics and explosives, *J. Mater. Chem. C*, 2017, **5**(33), 8469–8474, DOI: 10.1039/C7TC02885G.

105 J. Song, M. Huang, X. Lin, S. F. Y. Li, N. Jiang, Y. Liu, H. Guo and Y. Li, Novel Fe-based metal-organic framework (MOF) modified carbon nanofiber as a highly selective and sensitive electrochemical sensor for tetracycline detection, *Chem. Eng. J.*, 2022, **427**, 130913, DOI: 10.1016/j.cej.2021.130913.

106 Y. Zhang, B. Li, X. Wei, Q. Gu, M. Chen, J. Zhang, S. Mo, J. Wang, L. Xue, Y. Ding and Q. Wu, Amplified electrochemical antibiotic aptasensing based on electrochemically deposited AuNPs coordinated with PEI-functionalized Fe-based metal-organic framework, *Microchim. Acta*, 2021, **188**, 8, DOI: 10.1007/s00604-021-04912-z.

107 Y. Song, M. Xu, X. Liu, Z. Li, C. Wang, Q. Jia, Z. Zhang and M. Du, A label-free enrofloxacin electrochemical aptasensor constructed by a semiconducting CoNi-based metal-organic framework (MOF), *Electrochim. Acta*, 2021, **368**, 137609, DOI: 10.1016/j.electacta.2020.137609.

108 B. Wang, B. He, R. Guo, Q. Jiao, Y. Liang, J. Wang, Y. Liu, W. Ren and Z. Suo, A competitive-type electrochemical immunosensor based on Ce-MOF@Au and MB-Au@Pt core-shell for nitrofuran metabolites residues detection, *Bioelectrochemistry*, 2021, **142**, 107934, DOI: 10.1016/j.bioelechem.2021.107934.

109 X. Niu, X. Bo and L. Guo, MOF-derived hollow NiCo2O4/C composite for simultaneous electrochemical determination of furazolidone and chloramphenicol in milk and honey, *Food Chem.*, 2021, **364**, 130368, DOI: 10.1016/j.foodchem.2021.130368.

110 Y. Q. Xue, X. Yang, X. L. Sun, Z. Y. Han, J. Sun and H. He, Reversible Structural Transformation of CuI-Tb(III) Heterometallic MOFs with Highly Efficient Detection Capability toward Penicillin, *Inorg. Chem.*, 2021, **60**(15), 11081–11089, DOI: 10.1021/acs.inorgchem.1c00952.

111 S. Wang, B. He, Y. Liang, H. Jin, M. Wei, W. Ren, Z. Suo and J. Wang, Exonuclease III-Driven Dual-Amplified Electrochemical Aptasensor Based on PDDA-Gr/PtPd @ Ni-Co Hollow Nanoboxes for Chloramphenicol Detection,

ACS Appl. Mater. Interfaces, 2021, **13**, 26362–26372, DOI: 10.1021/acsami.1c04257.

112 L. Zhu, G. Liang, C. Guo, M. Xu, M. Wang, C. Wang, Z. Zhang and M. Du, A new strategy for the development of efficient impedimetric tobramycin aptasensors with metallo-covalent organic frameworks (MCOFs), *Food Chem.*, 2022, **366**, 130575, DOI: 10.1016/j.foodchem.2021.130575.

113 E. Patyra, C. Nebot, R. E. Gavilán, K. Kwiatek and A. Cepeda, Prevalence of veterinary antibiotics in natural and organic fertilizers from animal food production and assessment of their potential ecological risk, *J. Sci. Food Agric.*, 2023, DOI: 10.1002/jsfa.12435.

114 J. Dong, P. Shen, S. Ying, Z. Li, Y. Yuan, Y. Wang, X. Zheng, S. Peh, H. Yuan, G. Liu, Y. Cheng, Y. Pan, L. Shi, J. Zhang, D. Yuan, B. Liu, Z. Zhao, B. Z. Tang and D. Zhao, Aggregation-Induced Emission (AIE)-Responsive Metal-Organic Frameworks, *Chem. Mater.*, 2020, **32**(15), 6706–6720, DOI: 10.1021/acs.chemmater.0c02277.

115 D. Wang and B. Z. Tang, Aggregation-Induced Emission Luminogens for Activity-Based Sensing, *Acc. Chem. Res.*, 2019, **52**(9), 2559–2570, DOI: 10.1021/acs.accounts.9b00305.

116 W. Cheng, X. Tang, Y. Zhang, D. Wu and W. Yang, Application of metal-organic framework (MOF)-based sensors for food safety: Enhancing mechanisms and recent advances, *Trends Food Sci. Technol.*, 2021, **112**, 268–282, DOI: 10.1016/j.tifs.2021.04.004.

117 S. Głowniak, B. Szczęśniak, J. Choma and M. Jaroniec, Mechanochemistry: Toward green synthesis of metal–organic frameworks, *Mater. Today*, 2021, **46**, 109–124, DOI: 10.1016/j.mattod.2021.01.008.

118 W. Li, Y. Li, W. Zhang, D. Yin, Y. Cheng, W. Chu and M. Hu, Size-controlled flow synthesis of metal-organic frameworks crystals monitored by *in situ* ultraviolet-visible absorption spectroscopy, *Chin. Chem. Lett.*, 2021, **32**(3), 1131–1134, DOI: 10.1016/j.cclet.2020.09.039.

119 L. Liu, Y. Zhou, S. Liu and M. Xu, The Applications of Metal-Organic Frameworks in Electrochemical Sensors, *ChemElectroChem*, 2018, **5**(1), 6–19, DOI: 10.1002/celc.201700931.

120 Y.-Z. Chen, Z. U. Wang, H. Wang, J. Lu, S.-H. Yu and H.-L. Jiang, Singlet Oxygen-Engaged Selective Photo-Oxidation over Pt Nanocrystals/Porphyrinic MOF: The Roles of Photothermal Effect and Pt Electronic State, *J. Am. Chem. Soc.*, 2017, **139**(5), 2035–2044, DOI: 10.1021/jacs.6b12074.

121 L. Wang, S. Li, Y. Chen and H. Jiang, Encapsulating Copper Nanocrystals into Metal–Organic Frameworks for Cascade Reactions by Photothermal Catalysis, *Small*, 2021, **17**(22), 2004481, DOI: 10.1002/smll.202004481.

122 R. P. Lakshmi, P. Nanjan, S. Kannan and S. Shanmugaraju, Recent advances in luminescent metal-organic frameworks (LMOFs) based fluorescent sensors for antibiotics, *Coord. Chem. Rev.*, 2021, **435**, 213793, DOI: 10.1016/j.ccr.2021.213793.

123 Q. Wang and W. M. Zhao, Optical Methods of Antibiotic Residues Detections: A Comprehensive Review, *Sens. Actuators, B*, 2018, **269**, 238–256, DOI: 10.1016/j.snb.2018.04.097.

124 G. Wei, Y. Lu, S. Liu, H. Li, X. Liu, G. Ye and J. Chen, Microplasma electrochemistry (MIPEC) strategy for accelerating the synthesis of metal organic frameworks at room temperature, *Chin. Chem. Lett.*, 2021, **32**(1), 497–500.

125 Q. Shao, X. Zhang, P. Liang, Q. Chen, X. Qi and M. Zou, Fabricate ion of magnetic Au/Fe_3O_4/MIL-101(Cr) (AF-MIL) as sensitive surface-enhanced Raman spectroscopy (SERS) platform for trace detection of antibiotics residue, *Appl. Surf. Sci.*, 2022, 153550.